NASA/CR—97-206215

Fatigue Reliability of Gas Turbine Engine Structures

Thomas A. Cruse, Sankaran Mahadevan, and Robert G. Tryon
Vanderbilt University, Nashville, Tennessee

Prepared under Grant NGT–51053

National Aeronautics and
Space Administration

Lewis Research Center

October 1997

Available from

NASA Center for Aerospace Information
800 Elkridge Landing Road
Linthicum Heights, MD 21090-2934
Price Code: A04

National Technical Information Service
5287 Port Royal Road
Springfield, VA 22100
Price Code: A04

FATIGUE RELIABILITY OF GAS TURBINE ENGINE STRUCTURES

Thomas A. Cruse, Sankaran Mahadevan, and Robert G. Tryon
Vanderbilt University, Nashville, Tennessee

Abstract

The results of an investigation are described for fatigue reliability in engine structures. The description consists of two parts. Part I is for method development. Part II is a specific case study. In Part I, the essential concepts and practical approaches to damage tolerance design in the gas turbine industry are summarized. These have evolved over the years in response to flight safety certification requirements. The effect of non-destructive evaluation (NDE) methods on these methods is also reviewed. Assessment methods based on probabilistic fracture mechanics, with regard to both crack initiation and crack growth, are outlined. Limit state modeling techniques from structural reliability theory are shown to be appropriate for application to this problem, for both individual failure mode and system-level assessment. In Part II, the results of a case study for the high pressure turbine of a turboprop engine are described. The response surface approach is used to construct a fatigue performance function. This performance function is used with the first order reliability method (FORM) to determine the probability of failure and the sensitivity of the fatigue life to the engine parameters for the first stage disk rim of the two stage turbine. A hybrid combination of regression and Monte Carlo simulation is to use incorporate time dependent random variables. System reliability is used to determine the system probability of failure, and the sensitivity of the system fatigue life to the engine parameters of the high pressure turbine. The variation in the primary hot gas and secondary cooling air, the uncertainty of the complex mission loading, and the scatter in the material data are considered.

Part I - METHODOLOGIES

Summary

Part I is a review of the development of reliability assessment methodologies for gas turbine engine structures. The essential concepts and practical approaches to damage tolerance design in the gas turbine industry are summarized. These have evolved over the years in response to flight safety certification requirements. The effect of non-destructive evaluation (NDE) methods on these methods is also reviewed. Assessment methods based on probabilistic fracture mechanics, with regard to both crack initiation and crack growth, are outlined. Limit state modeling techniques from structural reliability theory are shown to be appropriate for application to this problem, for both individual failure mode and system-level assessment. These are observed to provide useful sensitivity information on the influence of various engine parameters on the reliability.

Introduction

The reliability of a gas turbine engine structure is affected by the uncertainties in the operating environment (speed, temperature etc.) as well as in the structural properties (material properties, geometries, boundary conditions etc.). Traditional design methods generally account for these uncertainties using experience-based design safety margins. However, the statistical nature of fatigue and crack growth properties have long been recognized and given increasingly appropriate treatment. For example, a common commercial certification requirement is that the probability of crack initiation be less than 1/1000, recognizing the statistical basis of this problem.

Several methodologies have been developed during the past several decades to address the problem of fatigue and fracture reliability of gas turbine engine structures. These include crack initiation and crack growth models, non-destructive evaluation, probabilistic risk assessment etc. Recent years have seen the development of limit state modeling approaches to estimating component and system structural reliability, including advances in response surface, efficient simulation, and analytical approximation techniques. This paper summarizes the development of the various methods for fatigue reliability assessment, and the advances

made by the gas turbine engine industry in applying these concepts. The companion paper (Part II) [43] presents a case study in which the limit state modeling methodology is applied for individual crack as well as system-level assessment.

1 Damage Tolerant Design in the Aeropropulsion Industry

For the most part, engine design today is driven by safe life design philosophy — maximize the number of flight cycles before cracking can be expected. This has been largely successful over the years, especially in the commercial engine market, due to a very heavy emphasis placed on high performance materials, material quality control, and processing control. The lead organization for much of this was Pratt & Whitney, as they had 90% of the commercial market share in the 1960's and 1970's, when much of the production standards on the part of suppliers was established.

The FAA life-certifies critical rotating structures in engines, such as disks, shafts, spacers, and hubs. Some work is ongoing for life certifying static engine structures such as diffuser cases which see the same stress levels as many rotating parts and failure of which is every bit as critical. Two engine manufacturers certify the rotating parts on a minimum life basis, meaning that at the mandatory retirement life of the parts, a statistically very small sample of the parts can be expected to have initiated a crack. The U.S. Air Force refers to this safe life as the "economic life" of the part. Exposure to more flight cycles than this limit results in a rapidly increasing number of cracked parts. The design basis of these two life methods is different as Pratt & Whitney uses an empirical crack initiation model and Rolls Royce uses a fracture mechanics model for initiation.

Around 1980, the U.S. Air Force Systems Command began to develop the engine structural integrity program (ENSIP), patterned in appropriate ways after the successful ASIP standard. Much of the work in development of the ENSIP handbook [3] was validated through application to the Pratt & Whitney F-100 engine. Non-destructive evaluation (NDE) standards were reviewed, improved, and extended, as well as were the processes and process controls, as a result of that effort. All components received a detailed fracture mechanics analysis for NDE-sized flaws to determine the depot inspection intervals.

As a result of the durability review of the F-100 engine, it was found that the operating stress level and material crack growth rates in engine structures did not readily support damage tolerance. That is, the resulting depot level inspections would be required at uneconomically short intervals, based on the existing NDE capabilities. As a result, the San Antonio Air Logistics Center implemented cryogenic proof spin testing of the F-100 first stage fan, as well as elaborate, automated eddy current component inspection methods in order to establish highly sensitive NDE capabilities [26].

Very high strength turbine wheel designs in the 1970's started using powder metallurgy (PM) nickel base superalloys, such as the Pratt & Whitney IN100 and the General Electric René 95 alloys. Due to prior commercial experience with PM disk design, Pratt & Whitney established very stringent powder handling

and processing standards. Considerable emphasis was placed on characterizing the intrinsic defects in these materials, for example [19], in order to define more durable standards as well as to establish a fracture mechanics design basis for the materials. Again, this effort followed that in the commercial arena at Pratt & Whitney, but that commercial work was proprietary and still has not been adequately published.

The U.S. Air Force initiated an effort to increase the damage tolerance of powder metallurgy, nickel base superalloys. It was found that a coarsening of the grain structure resulted in slower crack growth rates. The trade-off was that the crack initiation life of the material decreased, thereby decreasing the economic life limits of the parts. Damage tolerance was selected as the more important design concern in the final material process selection.

Engine materials have high intrinsic strength and resulting fatigue capacity. This quality has always come with a price. For example, a single nickel superalloy disk may cost well in excess of $50K. The U.S. Air Force observed that there was much wasted money in the old method of retiring disks at an economic life limit, because so few might be expected to be cracked. As a result, the "retirement for cause" (RFC) philosophy of disk lifing was investigated [44], [22]. The RFC approach was to combine the inspection processes being developed by the damage tolerance requirements with an indefinite life limit of engine parts, such that a part stayed in service until it was found to be cracked; when cracked, the part was to be removed from service. Significant probabilistic fracture mechanics issues were uncovered in the RFC approach owing to the exposure and liability associated with missed cracks [44].

During this time period, the commercial engine fleets were setting the pace in terms of applied fracture mechanics of engine parts. Air Force and Navy engines were too few and acquiring cycles at too slow a rate to challenge the life envelope the way the commercial engines were. For example, significant numbers of mid-size commercial turbofan engines were first designed in the late 1950's and are still being sold (in updated versions, of course) today. There are thousands of such engines, each of which has a high stressed titanium fan disk, a high stressed nickel turbine disk, and multiple high stressed steel high pressure compressor (HPC) disks. The certified life limits on the various designs range from 15,000 flights to 20,000 flights. Some operators might accumulate in excess of 2,000 fatigue cycles a year.

Some design successes were clearly established by the commercial fleets. The titanium fan disks at Pratt & Whitney were retired in such numbers by the early 1980's that one had very high statistical confidence in the minimum fatigue life of the material. Equally high reliability was demonstrated for a number of turbine disk designs as well. However, there were also some design problems in the late 1970's and 1980's. It was found, for example, that the stresses in engine disks had not been adequately calculated in the early design periods, prior to the use of the finite element method. As a result, several engine models had disks which would not reach their initial design life. Damage tolerance assessments were made using probabilistic fracture mechanics to determine what inspection intervals could be imposed without undue risk to the total fleet operations of the affected engines.

The FAA accepted a probabilistic risk assessment (PRA) basis for an in-service, RFC program in order

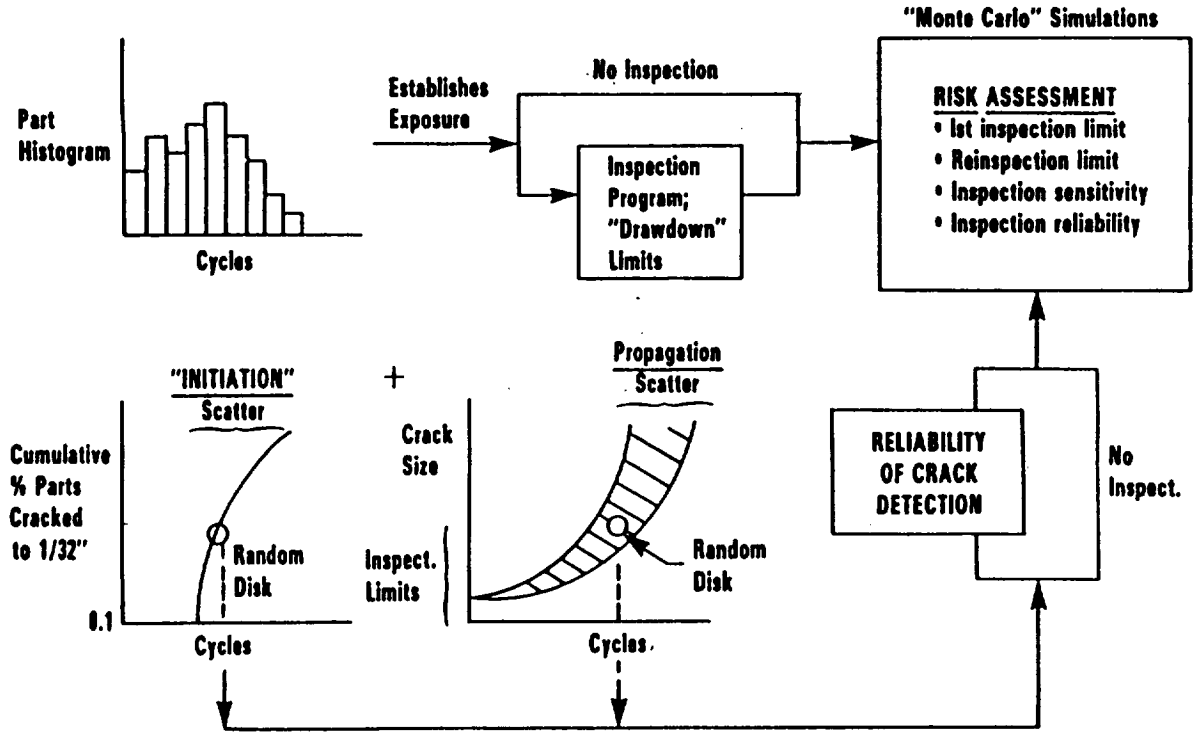

Figure 1: Probabilistic Risk Assessment Flow Diagram for Disk Cracking

to minimize the number of aircraft engines that had to be removed from service due to field cracking. The program was so successful that the FAA adopted the probabilistic risk assessment as the basis for all engine disk in-service cracking problems. The elements of the PRA shown in Figure 1 include probabilistic models for crack initiation, crack propagation, and NDE probability of detection (POD). The total fleet risk is obtained by summing the individual element risks over the entire fleet of engine disks using the known, current and future cyclic histogram. The inspection intervals are then adjusted in such a way to achieve the desired level of risk of disk failure for the total fleet.

Corrosion and multisite fatigue damage were found to be important elements of some of these in-service cracking problems. The corrosion occurs in cadmium plated, steel HPC disks. The multisite corrosion results in multiple crack origins. Figure 2 gives a notion of the multisite origins problem for a disk with multiple tie-rod holes, each of which has high stresses on the inside of the hole along the circumferential diameter of the hole.

The original PRA for this problem was based on the usual assumption of a single crack and a nominal sensitivity for the magnetic fluropenetrant NDE procedure then in use for the part. While the PRA was in effect, statistical reviews of the in-service crack size data strongly suggested that the fracture mechanics model was non-conservative and that the computed risk for the inspection program had to be adjusted upwards, meaning that there was a significant expectation of further field events of uncontained ruptures. A

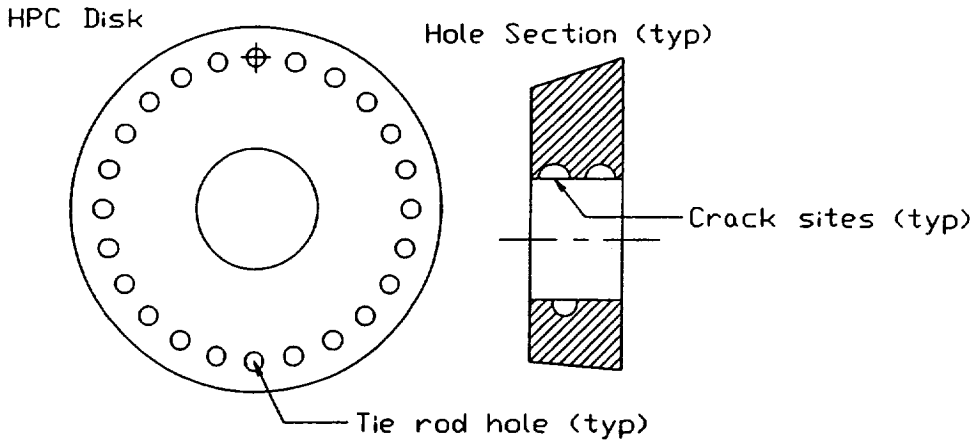

Figure 2: Typical HPC Disk with Multiple Corrosion-induced Fatigue Origins

review of the failed hardware from several incidents revealed that the multisite crack initiation process could give rise to reduced fracture mechanics lives.

Several cracking scenarios are shown for this problem in Figure 3, taken from that original unpublished work. The hardest part of the effort was to combine the factors of multisite cracking with the physical nature of the NDE method used, in that two small cracks close together were identified as one larger crack. An engineering approach was used for the problem by the first author and a critical combination of multiple crack spacings was used to define a new fracture mechanics model. The revised model was used with the Monte Carlo method to successfully simulate the in-service cracking data. Based on this success, the inspection intervals for the airline operators was reduced and no further incidents of disk failures were recorded.

In-service failure history involving the uncontained failure of more than a dozen mid-size commercial turbofan engines showed that the final failure event liberated a rim segment that usually contained three tie-rod holes and, less frequently, two tie-rod holes, as illustrated in Figure 4. While many holes (out of the 23 on each disk) had cracks, the failure occurred when multiple cracks linked up in the patterns indicated. Thus, multiple crack origins at multiple holes, crack growth from multiple origins, multiple crack link-up of two-hole and three-hole patterns, and growth of the final cracks to the rim defined the probabilistic field cracking pattern for this in-service problem.

Later designs of large-size commercial turbofan engines made use of rotor designs that eliminated the tie-rods holding the stack of engine disks together. Instead, the rotors were assembled by bolting disks one to another, near the outer diameter of the rotors. This lighter design concept resulted in much more shell-type bending of the disks. However, a new multisite fatigue origin problem was discovered. Shell bending of rotor disks causes high local stresses to occur around the full circumference of the disk, at the peak stress locations. A simple diagram is included to try and clarify the locations of these origins in Figure 5.

Today's engine designs make use of welded rotor construction with the welds placed in low stress locations

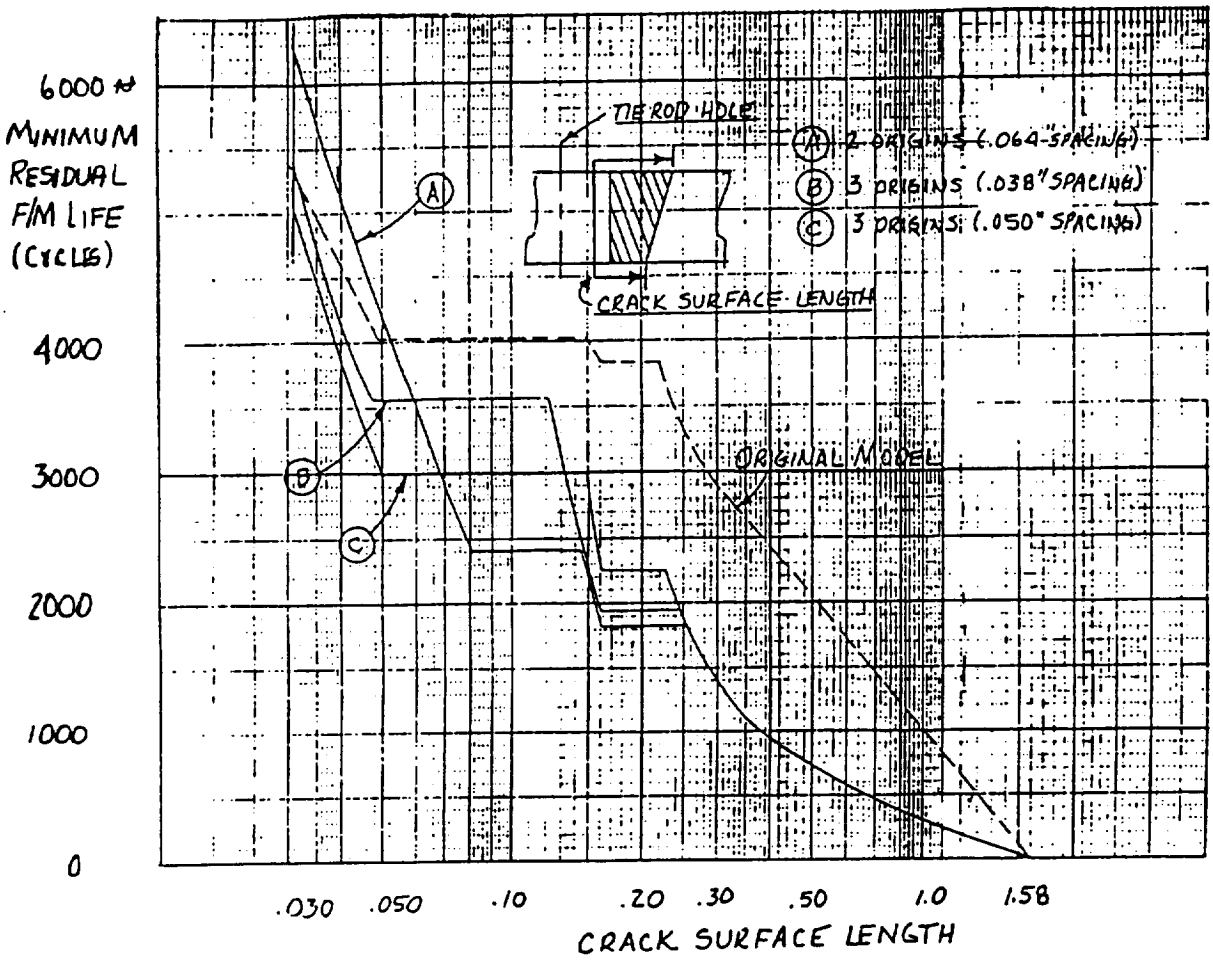

Figure 3: Various Residual Life Models for multisite Tie-Rod Hole Cracks

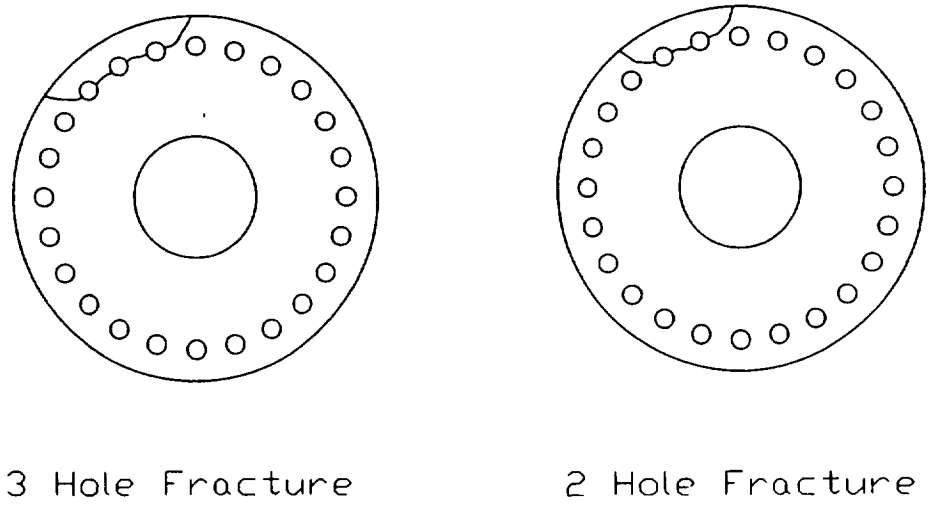

Figure 4: Multi-hole Fatigue Cracks Associated with In-service Failures

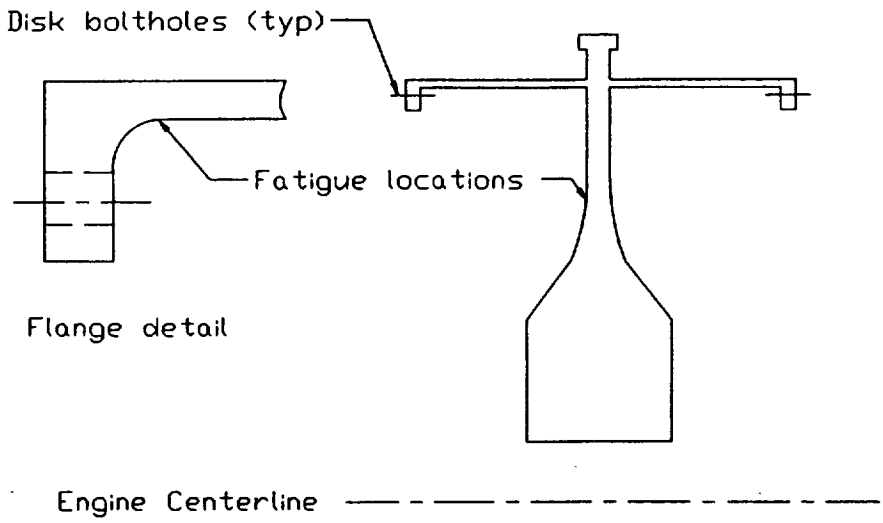

Figure 5: Typical HPC Disk with Local Bending Stress Concentrations

for damage tolerance. However, these rotors are even more light-weight and are susceptible to this same bending stress-induced multi-site damage.

In all of the commercial gas turbine engine in-service cracking problems, probabilistic damage tolerance analysis plays an absolutely crucial role. When an in-service cracking problem occurs that affects multiple engines, the FAA manages the problem through the legal control of an airworthiness directive which mandates repetitive field inspections of cracked components in order to assure that no commercial engine is flying with a significant sized crack. The alternative of grounding all suspect engines until replacement parts are available is untenable. The FAA accepted and now requires that this field cracking problem be managed using probabilistic fracture mechanics and risk assessment. Retirement-for-cause is therefore a reality for these problems, and depends not only on fracture mechanics analysis, but on the technology of crack detection.

An intrinsic part of the damage tolerance approach to life management is the effective use of non-destructive evaluation (NDE) or inspection (NDI). The NDE issues include the sensitivity of the method (the minimum, nominal detectable crack size), and the reliability of detection (usually given in terms of the POD). A key reliability question for NDE measures is, what is the largest crack that can be missed? A related, supporting issue for NDE is automation, as NDE reliability is often really an operator-specific issue which can only be controlled through the use of automation. For a recent review on the subject, see [24].

Engine field reliability and life extension are most often driven by the number of operational cycles to generate a crack that is detectable by standard NDE methods. Past experience, with one notable exception, has been based on the nominal sensitivity level of the NDE method. For problems with relatively few components to inspect, the nominal sensitivity is adequate to define the inspection intervals.

However, for problems with many inspections — many components, or many repetitions — the POD characteristic for the NDE method is critical. The true POD characteristic for an NDE method is the hardest and least well developed element in the overall damage tolerance approach to in-service cracking management. The most important and most difficult issue is to provide the NDE specialist with a realistic sample of the critical defects that are to be detected with reliability. Too often, the NDE specialist is faced with the task of setting field inspection limits on the basis of a laboratory induced fatigue crack or corrosion condition; such laboratory defects rarely, if ever, represent the true state of an in-service crack[35]. It is only after a field problem has been active for some time that real cracks can be examined. The question of what is the largest undetectable crack is often determined after the failure.

2 Probabilistic Fracture Mechanics

2.1 Probabilistic Crack Initiation Modeling

Fatigue crack initiation is a complex process involving many metallurgical and defect related issues. The crack initiation process occurs in a very small volume and is therefore greatly influenced by the microstructure of the material. Typically, crack initiation is loosely correlated to macro-stresses and strains. The most successful approaches to deterministic fatigue crack initiation are empirical in that various algebraic functions of damage driving parameters are combined through some damage summation algorithm and fitted to experimental data. These models give no relationship between the microstructural features of the material and the crack initiation process.

Until relatively recently, the fatigue damage process was not tied to a well-defined state of damage which, generally, is a defined crack size. Rather, the cycles to specimen failure were reported. So long as one is performing material characterization testing only and not developing a design database, specimen failure provides a cheap way to assess relative fatigue lives for various materials. Even then, however, the role of machining the specimens for various materials is not characterized. Again, the generalization of the results to design is thereby compromised.

Research into fatigue crack initiation for the U.S. Air Force by Cruse and Meyer [14, 15] included titanium and nickel alloys. The goal was to define the role of the mechanical factors in notches that governed fatigue crack initiation to a specified crack size. The goal could only be met by eliminating or minimizing extraneous factors to arrive at the best mechanical model. Specimens were taken from single heats of the two selected materials, all surface preparations were closely controlled to design specifications for machined features such as finished holes, and replication was used to define the cycles to a given crack size. Zero stress, unnotched ($K_T = 1$), strain-controlled specimens were considered the baseline material specimen; all machined specimens were taken to be in an altered mechanical state whose parameters had to be included in the life model.

The results of the test program confirmed that the scatter in fatigue lives for these controlled LCF tests was much less than the design basis for scatter and that sub-component fatigue behavior was significantly altered by the machining operation. However, it did appear that one could map the data for unnotched specimens to that for sub-components through a macromechanical model of the local stress and strain conditions (each of these specimens failed due to surface crack initiation; sub-surface defects are obviously not similarly affected).

Such an approach to fatigue life characterization seeks to define the expected value of the fatigue strength of the material. For example, the life model that was used included both cyclic strain range $\Delta\epsilon$ and mean stress σ_M parameters in the simple power law form

$$N = A\Delta\epsilon^b 10^{C\sigma_M} \tag{1}$$

There are two statistical approaches to using a life model such as in Eq. 1. The approach most often used in design is to construct a lower bound for the parameter A based on a design basis (e. g., Type A or B; mean minus 3σ). Such an approach is not particularly good for a probabilistic life modeling. The more proper approach is to define a probability model for life and characterize the life scatter through the probabilistic parameters. (Note: For simplicity, the discussion herein will focus on the simplest of probabilistic fatigue models, those for which the load history can be described deterministically. There is a rich literature available for the treatment of fatigue as a random process, for example see [42] and references therein and [7].)

Two probability models are most widely used for fatigue design, the Weibull and the lognormal distributions. There are advantages and disadvantages to both models. The Weibull distribution was developed on the basis of a mechanical model for fracture (fatigue) and yielding of materials [50]. There are three characteristics of the Weibull distribution that make it useful in fatigue modeling:

- the model has an increasing hazard rate indicating wear-out
- the model has a volume effect such that larger specimens have lower lives
- the model has three parameters such that minimum life can be included

The original size effect postulated by Weibull was that of a chain whose strength was defined by the strength of the weakest link. An extensive discussion of various methods to characterize Weibull size effects is available [27, 28]. A more mathematical approach to the size effect issue is given in [33].

However, the Weibull model is really most physically linked with the fracture of brittle materials due to existing defects, rather than with fatigue lifetime. The fact that the simple form of most fatigue models leads to linear life lines on a log-log plot makes the lognormal distribution the most convenient of the two. When plotting fatigue data on a log-log plot, the statistical distribution of the life data would be normal or Gaussian. The lognormal distribution also has the ability to have three parameters, thereby also allowing a minimum fatigue life capability. An example of this fairly standard application of the lognormal probability distribution to fatigue crack initiation is the work by Wirsching and his co-workers, e.g., [32].

The second approach, which is becoming more popular for modeling fatigue crack initiation, is the use of fracture mechanics as the empirical form of the life model. It is assumed in this approach that the fatigue crack initiation process is characterized by a single crack from an "equivalent initial flaw size (EIFS)," to use the terminology most often applied. This approach has been widely and effectively applied to aluminum aircraft structures by Yang and his co-workers. There exists now an extensive literature stemming form this work done in the 1980's.

An overview of the EIFS approach for aircraft is given in [51, 53]. The basic notion of the EIFS approach is to use probabilistic fracture mechanics in reverse, to take a given crack size — cycles distribution, and to back-calculate what distribution of initial flaws, growing as predicted by the fracture mechanics model, would correlate with the known data. If multiple load histories or multiple types of geometries all gave the same EIFS (which does not happen), then the EIFS would not be "equivalent" but would be intrinsic. As stated by Yang and his co-workers, the EIFS is an effective engineering tool which may produce more consistent life results than that obtained using purely empirical fatigue life models. Certainly, a fracture mechanics approach does allow a direct calculation of size effects if one can determine the volumetric distribution of the EIFS.

However, it is important to point out that the EIFS models in the literature are not tied to microstructure or to small flaw behavior. It is also important to point out that there is no probabilistic fatigue crack initiation model that specifically focuses on the nature of multi-site damage. As discussed in [4], the FAA Advisory Circulars on the subject state that a two-lifetime full-scale fatigue test is to assure that the probability of MSD is low.

2.2 Probabilistic Fracture Mechanics Modeling

This subject is the single most well defined application of probability methods in all of mechanical system reliability. An example of the scope of the previous work is found in the book on the subject [36]. A review of probabilistic crack growth modeling and probabilistic micromechanics for crack growth in the first chapter by the book's editor suggests the use of the lognormal model for probabilistic crack growth modeling because it is simple to use and conservative. Palmberg et al. [35] cite various works evaluating the various probability models and that lack of a significant statistical difference between them.

In fact, almost all probabilistic implementations of the standard form of fracture mechanics models do use the lognormal form, for example [4, 53, 34], and many others including most of the studies reported in [36]. The usual lognormal form of the probabilistic crack growth modeling is illustrated by using the Paris-form of the crack growth model, as follows

$$da/dN = C\Delta K^n \tag{2}$$

where n is usually taken to be deterministic and C is taken to be lognormally distributed (Note: While n may be taken to be random, the consensus is that one is able to reconstruct the original database of crack

growth data with excellent correlation by taking n to be deterministic; this is certainly far easier for what we are now describing). Taking the log of Eq. 2, we obtain

$$\log\{da/dN\} = \log C + n \log \Delta K \tag{3}$$

Each of the terms in Eq. 3 is now a normally distributed variable. The equation can be integrated analytically, if we take the initial flaw size to be quite small, the toughness to be deterministic, and the cyclic stress to be constant. When these are true, then the fatigue life is lognormally distributed. Of course, these are rarely useful and appropriate approximations and other methods must be used to determine the probability distribution for the fracture mechanics fatigue life. The most common method for computing the random fracture mechanics life in the general case is the use of Monte Carlo simulation, e.g., [5, 8, 2, 34].

Probabilistic fracture mechanics has been used in the design of titanium, steel, and nickel disks with internal defects since the early 1970's [16]. Figure 6 shows a set of design curves for a defined reliability of 0.999, where the curves represent differing statistical parameters for the subsurface defect, defect size, and material toughness. The material crack growth rate is taken to be lognormal with the usual level of material scatter for these alloys. The use of this type of design system has been effective in preventing the failure of titanium fan disks due to intrinsic, type-I hard-alpha defects. Such a design system can be directly couple to the sensitivity and reliability of the NDE methods used for detecting the subsurface defects.

A philosophically different approach to probabilistic fracture mechanics is based on various implementations of the Markov chain approach to simulating random processes, e.g. [42]. The thinking behind this approach is that if you look at the very local processes of crack growth, they appear to be random regarding whether or not the crack grows in a given cycle and which way it grows. The Markov chain modeling approach allows the current event to be random in a manner that is variable tied to the past history. For example, the current increment in crack extension could be totally random or it could be somewhat dependent on the current state. While the Markov chain approach seems at one level to mimic the observations of crack growth, it has no significant relation to the physics of the process. The start-stop randomness in crack growth is microstructural in nature and any simulation of this process must attempt to be microstructural in nature; such capability appears to be beyond the current state-of-the-art of microstructural fracture mechanics. The Markov chain models need extensive (and generally unavailable) statistical data on the crack jumping, and some non-physical solutions which the mathematical formulations allow. An example application of the Markov chain model with a microstructural flavor is given in [9].

The EIFS analysis described earlier also treats the crack growth process as a random process, [52], but in quite a different meaning. A summary of the method is found in [52]. In this approach, the crack growth rate is given as

$$da(t)/dt = X(t)L(\Delta K, K_{max}, R, S, a) \tag{4}$$

where $X(t)$ is a non-stationary random process with an expectation $E(X) = 1$. The function $L()$ defines the usual deterministic fracture mechanics model with a general retardation capability.

Yang et al. take $X(t)$ to be a lognormal random process. If we take $Z(t) = \log X(t)$, then the autocorrelation function for the random process in log-space is given as

$$R_{zz}(\tau) = E[Z(t)Z(t+\tau)] \tag{5}$$

Since the autocorrelation function in Eq. 5 is a function of τ only, the process is stationary. The Fourier transform of the autocorrelation function in Eq. 5, denoted $\Phi_{zz}(\omega)$, is the power spectral density of the lognormal random process. When the random process is completely correlated at any two time instants, then the random process $X(t)$ becomes a random variable X. The random crack growth process then becomes the lognormal random variable crack growth model, given by

$$\begin{aligned} da(t)/dt &= XQa^b(t) \\ a(t) &= \frac{a_0}{[1 - Xcta_0^c]^{1/c}} \end{aligned} \tag{6}$$

where $c = b-1$. In [53], the authors state that the fully correlated model in Eq. 7 gives the greatest dispersion of the various random process fracture mechanics models, where the fully random process model, Eq. 4, gives the least. Based on extensive evaluations using fractography data for various aircraft structures and configurations, the authors selected the lognormal, fully correlated approach. In this lognormal approach, the mean crack growth rate is a deterministic result; variance or crack growth dispersion is predicted as a function of time, based on fitting the model to the fractography results at one time point.

The EIFS approach has been applied to aircraft damage tolerance assessment for fastener holes [40, 51, 54]. Concern over the fact that the EIFS distribution depends on the sheet thickness and hole sizes is given in [35, pp. 64-65]. However, the method does seem to provide some quantitative means for assessing advanced alloy developments [29].

2.3 Limit State Modeling

Until recently, the two means for probabilistic fracture mechanics analysis were direct analytical solutions and Monte Carlo simulations. While the former is strictly limited to simple formulations, the latter is totally general and, in theory, provides the exact solution for any mathematical formulation. The practical limit of Monte Carlo though is for reasonable numbers of probabilistic variables, as the computer time — even today — is significant.

Approximate means for calculating probability integrals based on the first-order reliability method (FORM) began in the 1970's for the purpose of predicting the reliability of civil building structures. First-order refers to the use of a first-order Taylor series expansion of the physical system model in terms of the random variables. A performance function $g(X)$ is defined corresponding to a performance criterion in terms of limits on the physical system response variables (e.g., stress, natural frequency, fracture mechanics life), where X refers to the input random variables. The function $g(X)$ is defined such that a negative value corresponds to failure, positive value corresponds to safety, and $g(X) = 0$ is referred to as the limit state.

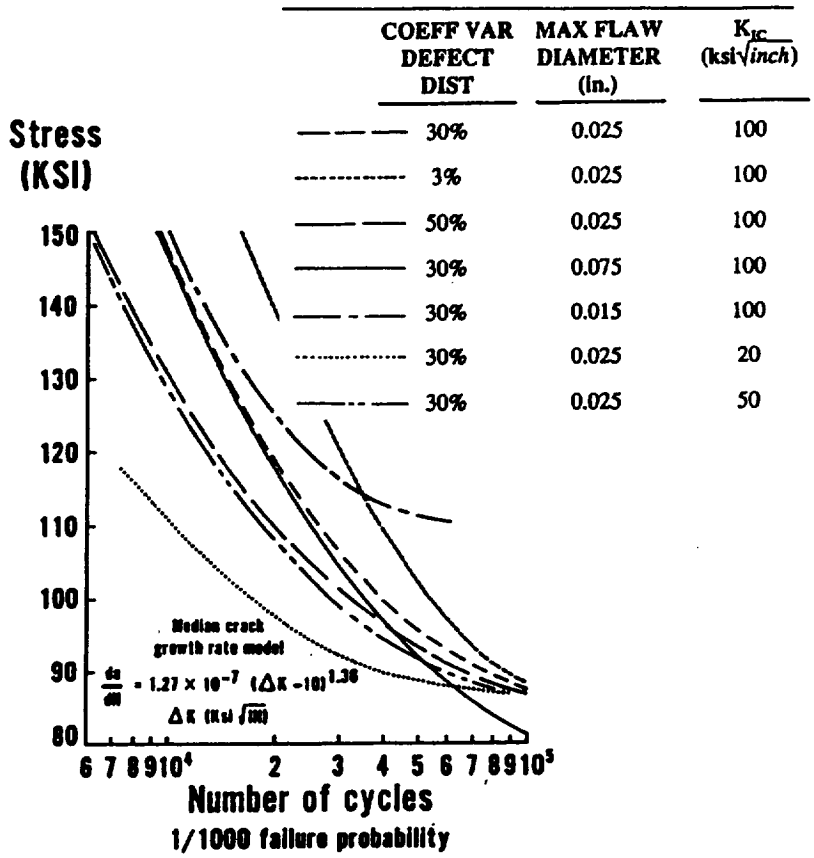

Figure 6: Fracture Mechanics Design Curves for Subsurface Defects

The first-order Taylor series expansion of $g(X)$ about the mean values (μ_i) of the random variables is given by

$$g(X) \approx \hat{g}(X) = a_0 + \sum_{i=1}^{i=N} \frac{\partial g}{\partial X_i}(X_i - \mu_i) \tag{7}$$

A safety index was first defined as $\beta = \mu_g/\sigma_g$ to quantify the reliability. μ_g and σ_g are easily obtained from the above equation. For uncorrelated, normal variables and linear performance functions, this results in the accurate estimate of the failure probabiity as $p_f = \Phi(-\beta)$. In general, however, and certainly in the case of probabilistic fracture mechanics, the function $g(X)$ is not linear and the random variables are not normally distributed and may not be uncorrelated. Nonetheless, the above first-order, second-moment representation served as the starting point for effective approximation algorithms developed later.

The probability of structural failure is mathematically defined as the integral of the joint probability density function $f_X(x)$ of all the random variables over the region where the limit state is violated, as

$$p_f = \int_{g(X)\leq 0} f_X(x)dx \tag{8}$$

The difficulty in evaluating the above multi-dimensional integral led to the development of approximate analytical methods such as FORM.

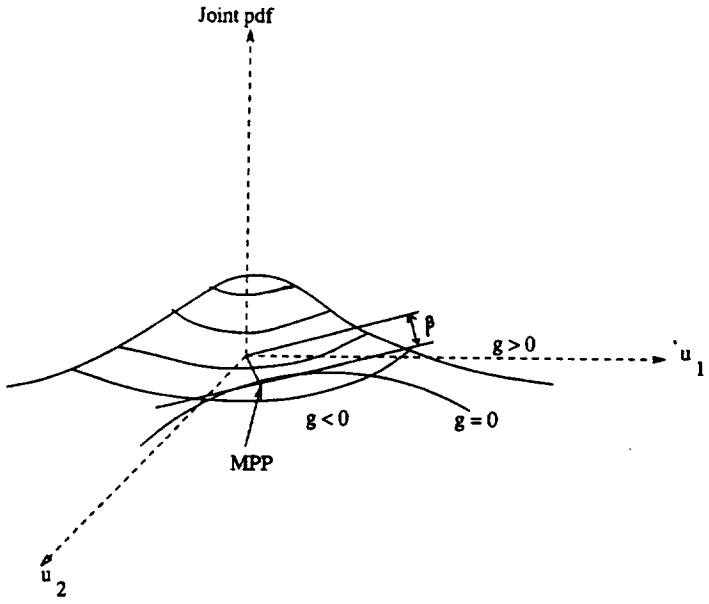

Figure 7: Failure Probability Estimation

A first-order approximation to the limit state is shown in Figure 7. The original variables (X) are all transformed to equivalent uncorrelated standard normal variables (u), and the closest point to the origin on the limit state is found. This minimum distance point is in fact the most probable point (MPP) of this limit state. A first-order estimate of the failure probability is obtained as [23]

$$p_f = \Phi(-\beta) \tag{9}$$

where β is the distance from the origin to MPP (referred to as the reliability index), and Φ is the cumulative distribution function of a standard normal variable. Thus the problem of multi-dimensional integration of the joint pdf in Eq. 8 is transformed to an optimization problem followed by a single dimensional integration of a normal pdf through linearization of the limit state surface at the MPP. Integration of the normal pdf is readily available.

Practical application of the above technique has to include random variables that may be correlated and non-normal. The correlated variables may be transformed to a set of uncorrelated variables through orthogonalization of their covariance matrix [1]). In the case of non-normal variables, it is advantageous to find equivalent normal variables, so that once again the MPP of the limit state can be found in the reduced normal space and Eq. 9 can be used. Such a transformation should result in a close approximation to the actual probability content in the failure domain. Two-parameter [37] and three-parameter [10, 47] transformations are available.

The NESSUS (Nonlinear Evaluation of Stochastic Structures Under Stress) computer code was developed at Southwest Research Institute under the leadership of NASA Lewis Research Center [12] to perform the

probabilistic analysis of select space shuttle main engine components. It uses the refined three-parameter equivalent normal transformation scheme of Wu and Wirsching [47]. However, instead of performing many iterations to search for the exact minimum distance point, NESSUS employs an Advanced Mean Value (AMV) procedure [49] to obtain sufficient accuracy in the second iteration. The search begins by computing the sensitivities of the performance function at the mean values of the random variables, and using these sensitivities to obtain a mean value first order (MVFO) estimate of the MPP and failure probability. Reanalysis at this point provides the correct value of the performance function at this point. This information, combined with that from the MVFO analysis, is seen to provide an accurate AMV estimate of the failure probability. Further refinements are also possible, if necessary. The AMV analysis has been verified for numerous problems using Monte Carlo simulation and has been found to provide accurate and fast estimates of failure probability for practical space shuttle main engine (SSME) hardware [11] [38].

Perhaps the most significant contribution of the limit state modeling technique is the computation of sensitivities of structural reliability to the basic random parameters. The sensitivity of the reliability index β to the original random variables X_i can be computed as

$$\frac{\partial \beta}{X_i} = \sum_{j=1}^{n} \frac{\partial \beta}{\partial u_j} \frac{\partial u_j}{\partial X_i} \tag{10}$$

where u_j's are the equivalent uncorrelated standard normal variables. The first term in the summation is obtained from the direction cosines of the MPP vector, and the second term is obtained from the transformation from the X-space to the u-space. This sensitivity measure combines both the physical sensitivities and the uncertainty of the random variables.

As part of the aforementioned NASA-funded research, the Rocketdyne Division of Rockwell International performed probabilistic analysis of a series of SSME structural analyses [38]. One of the components is the turbine blade from the turbopump for the engine, shown in Figure 8. The first-order solutions were performed using a developed finite element program which uses a fast numerical perturbation algorithm to obtain the first-order terms in the Taylor series expansion. The problem was analyzed using 18 random variables which represented an integrated systems analysis of the causes of stress uncertainty at all locations in the blade. One of the probabilistic results from that analysis is shown in Figure 9 which shows the probability for effective stress at a fatigue critical location in the blade. Also show in the figure is a table of the five most important of the 18 independent random variables. Two of the most important factors are single crystal orientation, one is a manufacturing variable, and two are system level engine performance variables. The general finite element analysis approach used in this study is given in [17].

Advanced reliability methods have been successfully used to predict the uncertainty in fracture mechanics lives of various types of structures and structural applications. A basic reliability-index (β) approach for fatigue critical offshore structures [21] shows that these reliability computations can be integrated into inspection criteria. The first-order and second-order method have been successfully applied to a stationary random process simulating aircraft loading history [48], to a fast-breeder reactor design [39], and to a steam

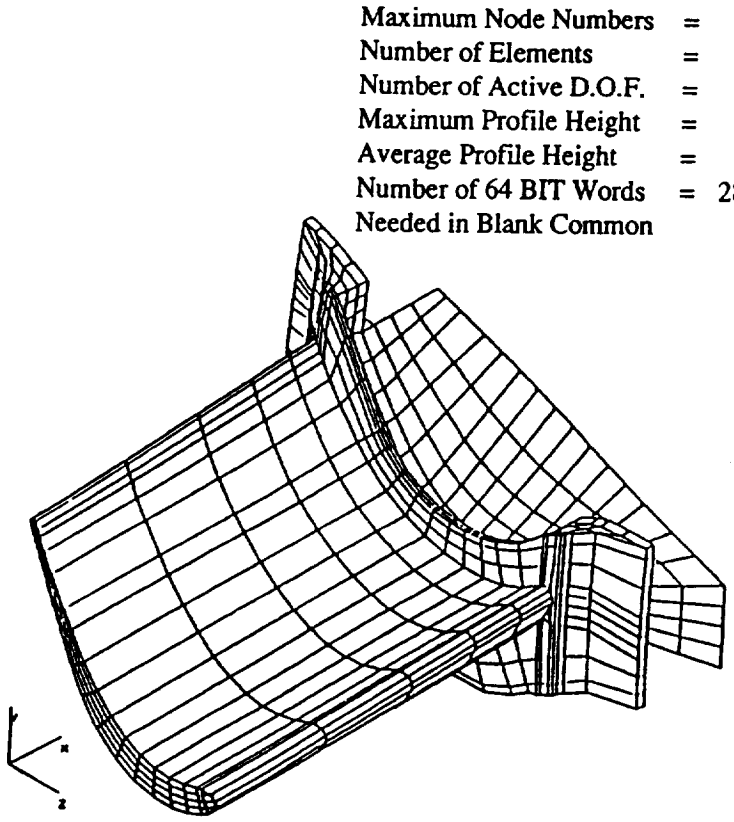

Figure 8: Turbine Blade Probabilistic Analysis

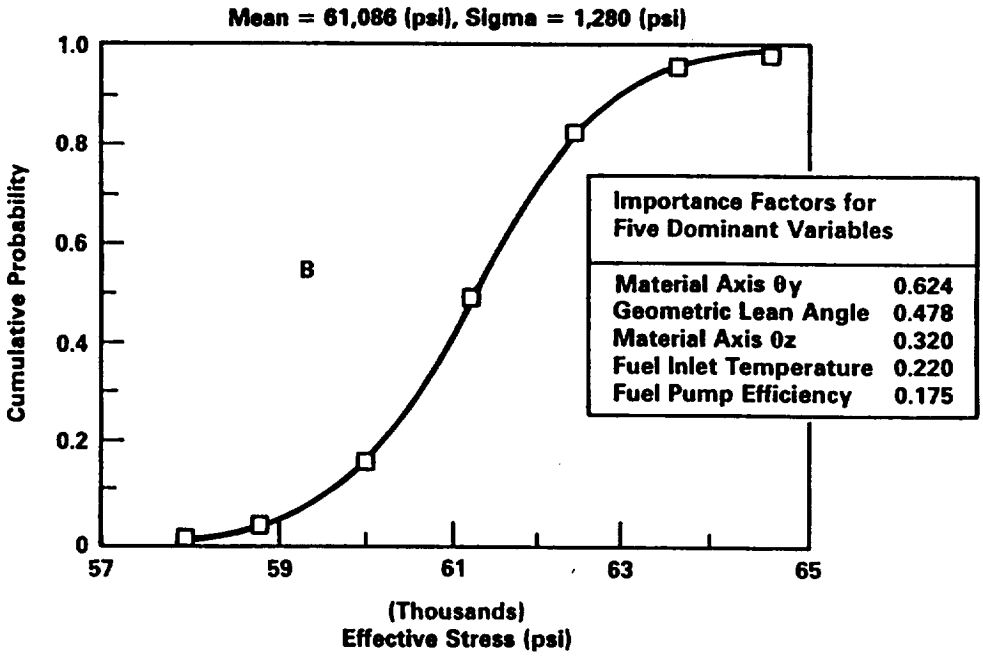

Figure 9: Blade Stress CDF and Probabilistic Sensitivity Factors

turbine design [41]. A summary of an updating algorithm to improve solution accuracy developed by the NASA-funded research [49] was shown to be effective for fracture mechanics analysis [45]. A special finite element approach to probabilistic fracture mechanics is given in [6] which is also based on the limit state approach.

Part II of this paper describes in detail the application of the limit state modeling methodology to the engine structures fracture reliability problem.

3 System Failure

The probabilistic estimation of fracture life of mechanical components also has to contend with issues such as multiple possible sites of crack initiation, the rate at which the initiated cracks grow at different sites, the probability of coalescence of two or more cracks, several possible crack propagation paths, etc. This becomes a system reliability problem.

Traditionally, mechanical system reliability has been based on classical statistics and experimental observations, and concepts such as MTBF and Weibull or exponential life distribution. In addition to the inadequacies of such an approach in linking component and system reliability to design decisions, increasingly complex propulsion systems are making it uneconomical to continue this approach due to the high cost involved in testing. Therefore the limit state modeling approach has been extended by the authors to system reliability evaluation of gas turbine engine structures. System failure may occur due to a combination of any of the individual component failure modes. Structural system reliability analysis has traditionally modeled structures as networks of simple parallel and series components analogous to electrical circuits. A "series" or weakest-link system is one in which the violation of any one of the design limit states causes system failure. In this case, the probability of system failure is computed through the union of the individual failure events. A "parallel" or redundant or fail-safe system is one in which system failure occurs only when all the individual modes are violated. In this case, the probability of system failure is the probability of joint occurence (intersection) of all the individual failure events.

For systems with a large number of components, it is difficult to accurately compute the joint probabilities of three or more failure events, except through Monte Carlo simulation. Therefore, first-order and second-order analytical bounds for the system failure probability have been derived, e.g., [18]. First-order approximations to the joint probabilities of multiple failure events have also been derived [20]. Monte Carlo simulation has been the tool of choice for large complex systems which consist of many components and failure paths. Efficient sampling schemes have been developed in this regard [25, 46].

System reliability estimation of mechanical structures such as in gas turbine engines also has to consider the fact that some failure modes such as yielding, fracture, creep etc. are progressive in nature and distributed over a continuum. Some of the failure modes may be physically related to each other; in that case the probability of failure in one mode as the structure undergoes progressive damage in another is of concern.

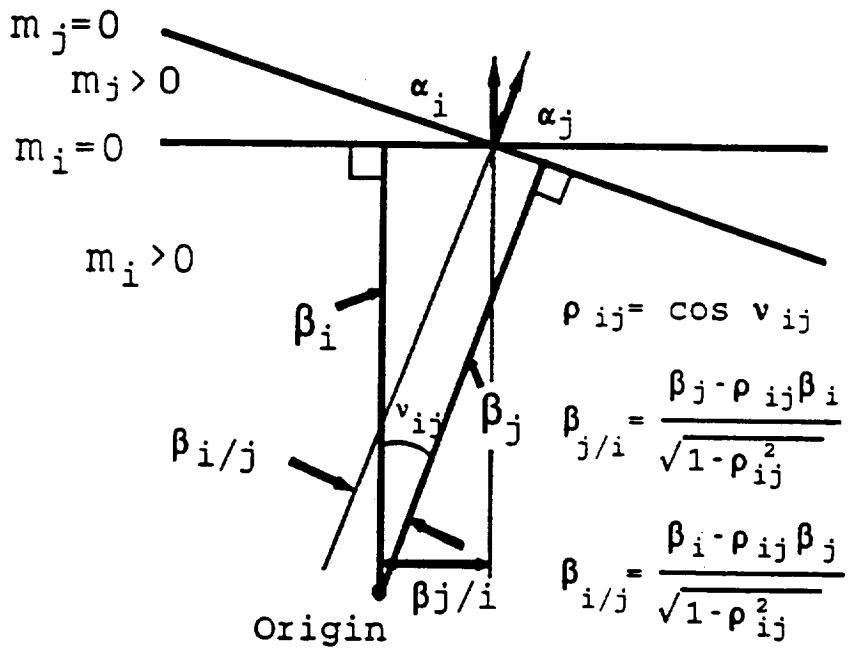

Figure 10: Joint Probability of Two Failure Modes

A structural reanalysis procedure has recently been developed to accurately estimate the failure probability various critical failure modes affected by progressive damage [13, 31].

System reliability analysis with the limit state modeling approach also results in the computation of overall system sensitivities to the random variables. For example, a first-order approximation to the system sensitivity factors may be computed as

$$\frac{\partial p_f^s}{\partial X_j} = \sum_{i=1}^{m} \frac{\partial p_f^i}{\partial X_j} \tag{11}$$

where p_f^s is the overall system failure probability, p_f^i is the ith mode failure probability, X_j is jth random variable, and m is the number of individual failure modes. This result applies to the case where the system failure is the union of the individual failures, and is based on the chain rule of differentiation applied to the first-order upper bound of the probability of the union.

The method described above provides accurate system reliability and sensitivity results for linear limit states. However, if the limit states are nonlinear, the joint probability region is different, as illustrated by Fig. 11. In such cases, one needs to find the exact intersection between the two limit states and then estimate the joint probability by constructing linear approximations to the limit states at this intersection, which may be referred to as a joint MPP. The problem of finding the correct joint MPP is one of constrained minimization. The well-known Rackwitz-Fiessler algorithm [37] has been extended to determine the joint MPP of two nonlinear limit states as outlined in [30].

Part II of this paper applies the system reliability methodology to determine the fatigue reliability of a two-stage high pressure turbine engine.

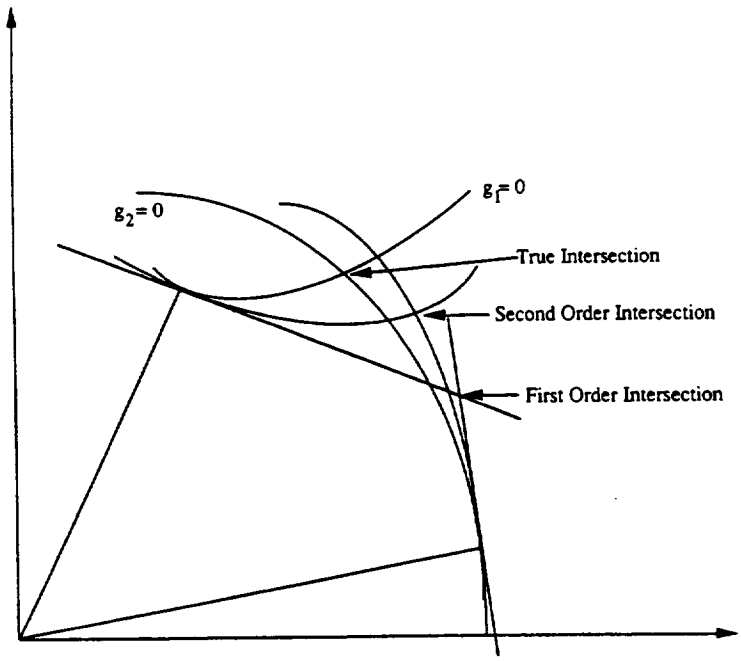

Figure 11: Two Nonlinear Limit States

Summary

This paper presented several methodologies to assess the fatigue fracture reliability of gas turbine engine structures. Major industry and government research efforts to develop practical damage tolerance design methods for commercial engines were outlined. The development and contribution of probabilistic fracture mechanics models for both crack initiation and crack growth were also discussed. The limit state modeling approach is an important recent method for both individual crack and system-level assessment. This is observed to provide important sensitivity information regarding the influence of the basic engine parameters on the fatigue reliability. Part II of this paper develops in detail the practical strategies and methods required to apply the limit state modeling to this problem [43]. An example application to a two-stage high-pressure turbine engine is presented therein to perform both individual crack and system-level fatigue reliability assessment.

Acknowledgments - This work was partially supported by NASA contract NAS3-24389, Lewis Research Center, Dr. C. C. Chamis, Program Manager.

References

[1] A. H.-S Ang and W. H. Tang, **Probability Concepts in Engineering Planning and Design, Vol 2,** John Wiley and Sons, New York, 1984.

[2] Anon., "Probabilistic/Fracture-Mechanics Model for Service Life", NASA Tech Briefs MFS-27237.

[3] Anon., U. S. Air Force, Military Standard MIL-STD-1783, 1984.

[4] Hiroo Asada, "Reliability assessment of pressurized fuselages with multiple-site fatigue cracks", **Proceedings of the 5^{th} International Conference on Structural Safety and Reliability**, 1989, pp. 2369–2372.

[5] P. M. Besuner, "Probabilistic fracture mechanics", in **Probabilistic Fracture Mechanics and Reliability**, ed. J. W. Provan, op. cit., pp. 387–436.

[6] G. H. Besterfield, W. K. Liu, M. A. Lawrence, and T. B. Belytschko, "Brittle fracture reliability by probabilistic finite elements", **Journal of Engineering Mechanics, Vol. 116**, No. 3, ASCE, 1990, pp. 642–659.

[7] V. V. Bolotin, "Theory of extremes and its applications to mechanics of solids and structures", **Proceedings of the 1^{st} World Congress of the Bernoulli Society**, Tashkent, USSR, ed. by Yu. A. Prohorov and V. V. Sazanov, Utrecht, The Netherlands, VNU Science Press, 1987.

[8] A. Brückner, "Numerical methods in probabilistic fracture mechanics", in **Probabilistic Fracture Mechanics and Reliability**, ed. J. W. Provan, op. cit., pp. 351–386.

[9] A. Brückner-Foit, H. Jäckels, H. Lahodny, and D. Munz, "Fatigue reliability of components containing microstructural flaws", **Proceedings of the 5^{th} International Conference on Structural Safety and Reliability**, 1989, pp. 1499–1506.

[10] X. Chen and N. C. Lind, "Fast Probability Integration by Three-Parameter Normal Tail Approximation",**Structural Safety, Vol. 1**, pp. 269-276, 1983.

[11] T. A. Cruse, O. H. Burnside, Y.-T Wu, E. Z. Polch, and J. B. Dias, "Probabilistic Structural Analysis Methods for Select Space Propulsion System Structural Components (PSAM)", **Computers and Structures, Vol. 29(5)**, pp. 891-901, 1988.

[12] T. A. Cruse, C. C. Chamis, and Millwater, H.R., "An Overview of the NASA(LeRC)-SwRI Probabilistic Structural Analysis (PSAM) Program", **Proceedings, 5th International Conference on Structural Safety and Reliability (ICOSSAR)**, San Francisco, California, pp. 2267-2274, 1989.

[13] T. A. Cruse, Q. Huang, S. Mehta, and S. Mahadevan, "System Reliability and Risk Assessment," **Proceedings of the 33rd AIAA/ASME/ASCE/AHS/ASC Conference on Structures, Structural Dynamics and Materials**, Dallas, Texas, pp.424-431, 1992.

[14] T. A. Cruse and T. G. Meyer, "A cumulative fatigue damage model for gas turbine disks subject to complex mission loading",**Journal of Engineering for Power, Vol. 101**, No. 4, 1979, pp. 563–571.

[15] T. A. Cruse and T. G. Meyer, "Low cycle fatigue life model for gas turbine engine disks", **Journal of Engineering Materials and Technology, Vol. 102**, 1980, pp. 45–49.

[16] T. A. Cruse, "Engine components", in **Practical Applications of Fracture Mechanics**, NATO AGARDograph #257, 1980, Chapter 2.

[17] T. A. Cruse, K. R. Rajagopal, and J. B. Diaz, "Probabilistic structural analysis methodology and applications to advanced space propulsion system components", **Computing Systems in Engineering, Vol. 1**, Nos. 2–4, 1990, pp. 365–372.

[18] O. Ditlevsen, "Narrow Reliability Bounds for Structural Systems", **Journal of Structural Mechanics, Vol. 3**, 453-472, 1979.

[19] N. Engsberg, C. G. Annis, Jr., and B. A. Cowles, **Effects of Defects in Powder Metallurgy Superalloys**, AFWAL-TR-81-4191, Feb. 1982.

[20] S. Gollwitzer and R. Rackwitz, "An efficient numerical solution to the multinormal integral", **Probabilistic Engineering Mechanics, Vol. 3(2)**, 1988, pp. 98-101.

[21] Guoyang Jiao and Torgeir Moan, "Reliability-based fatigue and fracture design criteria for welded offshore structures", **Engineering Fracture Mechanics, Vol. 41**, No. 2, 1992, pp. 271–282.

[22] J. A. Harris, Jr. and R. White, **Engine Component Retirement for Cause**, AFWAL-TR-87-4069, August 1987.

[23] A. M. Hasofer and N. C. Lind, "Exact and Invariant Second Moment Code Format", **Journal of the Engineering Mechanics Division, ASCE, Vol 100**, No.EM1, pp. 111-121, 1985

[24] Peter W. Hovey and Alan P. Berens, "Statistical evaluation of NDE reliability in the aerospace industry", **Review of Progress in Quantitative NDE, Vol. 7B**, 1988, pp. 1761-1768.

[25] A. Karamchandani, "Structural System Reliability Analysis Methods," Report No. 83, John A. Blume Earthquake Engineering Center, Stanford University, 1987.

[26] T. T. King, W. D. Cowie, and W. H. Reimann, "Damage Tolerance Design Concepts for Military Engines," **Proceedings No. 393, AGARD Conference on Damage Tolerance Concepts for Critical Engine Components**, 1985.

[27] P. Kittl and G. Diaz, "Five deductions of Weibull's distribution function in the probabilistic strength of materials", **Engineering Fracture Mechanics, Vol. 36**, No. 5, 1990, pp. 749–762.

[28] P. Kittl and G. Diaz, "Size effect on fracture strength in the probabilistic strength of materials", **Reliability Engineering and System Safety, Vol. 28**, 1990. pp. 9–21.

[29] P. E. Magnusen, A. J. Hinkle, W. T. Kaiser, R. J. Bucci, and R. L. Rolf, "Durability assessment based on initial material quality", **Journal of Testing and Evaluation, Vol. 18**, No. 6, 1990, pp. 439–445.

[30] S Mahadevan, and T. A. Cruse,"An Advanced First-Order Method for System Reliability", **Proceedings of the ASCE Joint Specialty Conference on Probabilistic Mechanics and Structural and Geotechnical Reliability**, Denver, Colorado, pp. 487-490, 1992.

[31] S. Mahadevan, T. A. Cruse, Q. Huang, and A. Mehta, "Structural Reanalysis for System Reliability Computation,"in **Reliability Technology**, ASME AD-28, ed. by T.A. Cruse, American Soc. of Mech. Engrs, New York, pp. 169-188, 1992.

[32] W. Scott Martin and Paul Wirsching, "Fatigue crack initiation - propagation reliability model", **Journal of Materials in Civil Engineering, Vol. 3**, No. 1, 1991, pp. 1–18.

[33] L. N. McCartney, "Extensions of a statistical approach to fracture", **International Journal of Fracture, Vol. 15**, No. 5, 1979, pp. 477–487.

[34] Liao Min and Yang Qing-Xiong, "A probabilistic model for fatigue crack growth", **Engineering Fracture Mechanics, Vol. 43**, No. 4, 1992, pp. 651–655.

[35] B. Palmberg, A. F. Blom, and S. Eggwertz, "Probabilistic damage tolerance analysis of aircraft structures", in **Probabilistic Fracture Mechanics and Reliability**, ed. J. W. Provan, op. cit., pp. 47–130.

[36] James W. Provan, Editor of **Probabilistic Fracture Mechanics and Reliability**, Martinus Nijhoff Publishers, Dordrecht, The Netherlands, 1987.

[37] R. Rackwitz and B. Fiessler, "Structural Reliability Under Combined Random Load Sequences", **Computers and Structures**, Vol. 9, No. 5, pp. 484-494, 1978.

[38] K.R. Rajagopal, A. Debchaudhury and J.F. Newell, "Verification of NESSUS Code on Space Propulsion Components", **Proceedings, 5th International Conference on Structural Safety and Reliability, ICOSSAR '89**, San Francisco, California, pp. 2299-2306, 1989.

[39] H. Riesch-Oppermann, and A. Brückner-Foit, "First- and second-order approximations of failure probabilities in probabilistic fracture mechanics, **Reliability Engineering and System Safety, Vol. 23**, 1988, pp. 183–194.

[40] J. L. Rudd, J. N. Yang, S. D. Manning, and G. W. Lee, "Probabilistic fracture mechanics analysis methods for structural durability", **Proceedings of AGARD Meeting on Behavior of Short Cracks in Airframe Components**, Toronto, Canada, 1982.

[41] Murari P. Singh, "Reliability evaluation of a weld repaired steam turbine rotor using probabilistic fracture mechanics", **Design, Repair, and Refurbishment of Steam Turbines, PWR-Vol. 113**, ASME, 1991, pp. 255–259.

[42] K. Sobczyk, "Stochastic models for fatigue damage of materials", **Advanced Applications of Probability, Vol. 19**, 1987, pp. 652–673.

[43] R. G. Tryon, S. Mahadevan, and T. A. Cruse, "Fatigue Reliability of Gas Turbine Engine Structures: Part II — Limit State Modeling", **Engineering Fracture Mechanics**, under review.

[44] T. Watkins, Jr. and C. G. Annis, Jr., **Engine Component Retirement for Cause: Probabilistic Life Analysis Technique**, AFWAL-TR-85-4075, June 1985.

[45] P. H. Wirsching, T. Y. Torng, and W. S. Martin, "Advanced fatigue reliability analysis", **International Journal of Fatigue, Vol. 13**, No. 5, 1991, pp. 389–394.

[46] Wu, Y.-T., "An Adaptive Importance Sampling Method for Structural System Reliability Analysis,"in **Reliability Technology**, ASME AD-28, ed. by T.A. Cruse, American Soc. of Mech. Engrs, New York, pp. 217-232, 1992.

[47] Y.-T. Wu and P. H. Wirsching, "New algorithm for structural reliability estimation", **Journal of Engineering Mechanics, Vol. 113**, No. 9, ASCE, pp. 1319–1336.

[48] Y.-T. Wu, O. H. Burnside, and J. Dominguez, "Efficient probabilistic fracture mechanics analysis", **Numerical Methods in Fracture Mechanics, Proceedings of the Fourth International Conference**, Ed. A. R. Luxmore, D. R. J. Owen, Y. P. S. Rajapakse, and M. F. Kanninen, San Antonio, Texas, 1987.

[49] Y.-T. Wu, H. R. Millwater, and T. A. Cruse, "An advanced probabilistic structural analysis method for implicit performance functions", **AIAA Journal, Vol. 28**, No. 9, 1990, pp. 1663–1669.

[50] W. Weibull, "A statistical distribution function of wide applicability",**Journal of Applied Mechanics, Vol. 18**, 1951.

[51] J. N. Yang, S. D. Manning, and J. L. Rudd, "Evaluation of a stochastic initial fatigue quality model for fastener holes", **Fatigue in Mechanically Fastened Composite and Metallic Joints, ASTM STP 927**, Ed. John M. Potter, American Society for Testing and Materials, Philadelphia, PA, 1986, pp. 118–149.

[52] J. N. Yang, W. H. Hsi, S. D. Manning, and J. L. Rudd, "Stochastic crack growth models for applications to aircraft", in **Probabilistic Fracture Mechanics and Reliability**, ed. J. W. Provan, op. cit., pp. 171–212.

[53] J. N. Yang and S. D. Manning, "Application of probabilistic approach for crack growth damage accumulation in metallic structures", **Proceedings of the 5^{th} International Conference on Structural Safety and Reliability**, 1989, pp. 1475–1482.

[54] J. N. Yang and S. D. Manning, "Demonstration of probabilistic-based durability method for metallic airframes", **Journal of Aircraft, Vol. 27**, No. 2, 1990, pp. 169–175.

Part II - A CASE STUDY

Summary

Part II focuses on a case study in which structural reliability-based methodologies are used to assess cyclic fatigue life. The study involves the high pressure turbine of a turboprop engine. The response surface approach is used to construct a fatigue performance function. This performance function is used with the first order reliability method (FORM) to determine the probability of failure and the sensitivity of the fatigue life to the engine parameters for the first stage disk rim of the two stage turbine. A hybrid combination of regression and Monte Carlo simulation is to use incorporate time dependent random variables. System reliability is used to determine the system probability of failure, and the sensitivity of the system fatigue life to the engine parameters of the high pressure turbine. The variation in the primary hot gas and secondary cooling air, the uncertainty of the complex mission loading, and the scatter in the material data are considered. The analysis incorporates standard modeling techniques used in the deterministic analysis of the fatigue life.

Introduction

The design of high performance gas turbine engines, aided by advanced materials with improved strength and temperature resistance, has made the overall turbine structural reliability often limited by the fatigue life of the high pressure turbine disks. Part I of this paper addresses the background and presents a review of modern gas turbine reliability methods [1]. The current paper develops a limit state modeling methodology to estimate gas turbine reliability. The methodology is applied to the high pressure turbine of a turboprop engine.

The fatigue life is measured by the useful number of flight missions and can be separated into two phases: crack initiation and crack propagation. Crack initiation life is the number of missions it takes for the crack to nucleate and grow to a size for which the laws of fracture mechanics apply. Crack propagation life is the number of missions from the initiation phase until the disk ruptures. Flight safety concerns make it

necessary to retire the disk before the fatigue life is exhausted. Retirement of the disk can be due to three causes:

1. Exceeding a predetermined number of missions,

2. Rejected at inspection due to exceeding a predetermined crack size, or

3. The undesirable event of rupture.

Gas turbine disks are subjected to complex thermo-mechanical loading with many uncertainties. The need for cost-effective designs has resulted in the development of probabilistic structural analysis tools to quantify the effects of these uncertainties on the fatigue life. Traditionally, direct analytical solutions which are limited to very simple models or computationally intensive Monte Carlo simulation techniques have been used to determine the probability of failure (P_f). This paper uses first order reliability methods (FORM) that not only compute the P_f for complicated models, but have the advantage of quantifying the sensitivity of the failure mode to the model parameters. The sensitivities are a useful tool for the designer to logically and systematically maximize the fatigue life of the system. The sensitivity analysis not only indicates which engine parameters are important, but also quantifies the importance. The FORM analysis uses regression analysis on standard engine model to develop the performance function. No new structural modeling techniques are required.

However, fatigue reliability analysis may also have to consider certain time-dependent variables. A discrete time-dependent event considered in this paper is a "bad start" in which the turbine experiences high temperature causing permanent residual stresses in the disks. The residual stresses produce accelerated crack growth for the remaining life of the disks. Therefore, the life of the disk is dependent on when the "bad start" occurs.

It is difficult to incorporate discrete time dependent variables in FORM and traditionally Monte Carlo methods have been used. However, since the temperature, stress, and crack growth models for a turbine disk are computationally intensive, such detailed models are not used directly in the Monte Carlo simulation in this paper. The Monte Carlo simulation incorporates computationally efficient, closed-form approximate equations developed from the same regression analyses used to develop the performance function in the FORM analysis.

FORM and hybrid Monte Carlo reliability analysis are applied to an individual failure mode in the rim of a first stage, integrally bladed high pressure turbine disk. The disk material is a cast nickel-base superalloy. The component experiences fatigue damage at the disk rim from mechanically and thermally induced loading. The mechanical loads are caused by the disk rotational speed. The thermal loads are caused by the temperature gradients through the disk. The loadings change with the mission cycle causing complex stress cycles in the disk.

The P_f of the overall high pressure turbine structural system is determined by first performing a FORM analysis on each of the individual failure modes. The individual FORM results are then used to determine

the system failure probability through the union of individual mode failures. The method also provides sensitivity information on the individual and system failure modes.

The approach presented considers the inherent scatter and the random nature of the engine operation, hardware and material data. The methodology can be described along the following steps:

1. Determine potentially significant random variables.
2. Use engine system and structural finite element models to determine temperatures and stresses.
3. Use crack initiation and crack propagation models to determine fatigue life.
4. Use FORM analysis to determine P_f and the sensitivities of individual failure modes (without time-dependent random variables).
5. Use hybrid Monte Carlo analysis to determine P_f of individual failure modes (with time-dependent random variables).
6. Use the system reliability method to determine P_f and the sensitivities of the system failure (without time-dependent random variables).

1 Performance Function

The performance function is generally defined as

$$g(\boldsymbol{X}) = f(X_1, X_2, \ldots, X_n) \tag{1}$$

where $g(\mathbf{X})$ is a closed form function of the random variables $X_1, X_2, \ldots, X_n$. The performance function representing the onset of fatigue in gas turbine engines, $g(\mathbf{X})$, is taken to be the number of flight cycles to failure. To develop the performance function, the potentially significant random variables must be identified. Perturbation analysis is performed to eliminate the random variables that do not significantly effect the fatigue life. Regression analysis is performed on the perturbation results to develop an closed form approximation to $g(\mathbf{X})$.

1.1 Determining Potentially Significant Random Variables

Ideally, all random variables should be measurable basic engine parameters. The random variables should be physically measurable, because the scatter must be known. The random variables should be primitive independent parameters such that the correlation between variables is minimized. The mean value, standard deviation, and distribution type must be estimated based on test data or sound engineering experience.

Although all physically measured parameters have some variability, some physically measured parameters can be considered deterministic variables while others must be considered random variables. A variable can

be considered deterministic if the range of variability is small enough such that any value within the range will not significantly affect the outcome of the modeled response. A variable must be considered random if range of variability is large enough such that changing the value within the range affects the response.

As a first step, engineering judgment should be used to determine which variable might be random. When in doubt, the variable should be considered random. Then a sensitivity analysis in which the response is modeled for the extreme values of the range of the variable in question should be performed. If the analysis shows the sensitivity to this variable to be low, then the variable can be considered deterministic. Care must be taken to reduce the number of random variables to as few as necessary because a major effort of probabilistic modeling is in determining the statistics of the random variables.

It is necessary to determine all of the engine parameters that affect fatigue life. In a complex system such as a gas turbine engine, it is quite difficult to understand the details as to which parameters affect disk life and exactly how these parameters interact. Detailed knowledge of each discipline and how each influences the disk response is needed. The disciplines that influence disk life include: primary hot gas flow, secondary cooling air flow, heat transfer, structural mechanics, life prediction, materials, inspection, failure analysis and design. Input from experienced engineers from all of the above disciplines was used to identify eleven potentially significant random variables. These included the burner outlet temperatures (BOT), burner profile, dwell times, seal clearances, material properties, and the number of missions at which the disk is retired. The following sections discuss the use of engine models to perform sensitivity analysis which showed the response to be sensitive to five of the eleven potentially significant random variables.

1.2 Engine Models

The present analysis incorporates the same basic engine models used in the deterministic fatigue life analysis. No new modeling techniques are needed. However, the models are combined in a manner that allows the designer to gain more understanding than what is available though a deterministic analysis. The basic models used in the analysis are briefly described below.

The factors that drive fatigue damage are the disk temperatures, stresses, and material properties. The disk temperatures are determined using both a 2-D finite element model and closed-form solutions which incorporate such variables as the temperatures, velocities, and pressures of the primary hot gas flow and secondary cooling air flow along with material thermal properties to determine the disk temperatures. Other variables such as the engine start-up idle time and shutdown idle time are included, along with disk geometry and seal clearances. Longer start-up and shutdown idle times affect the thermal loading by allowing the temperatures to stabilize, thus decreasing the thermal gradient between the disk bore and rim during the condition immediately following idle. Larger seal clearances affect the thermal loading by allowing more cooling air into the cavity. Figure 1 shows a schematic of the turbine along with some of the potentially random variables, namely burner outlet temperature (BOT), burner profile, gaps between rotating and

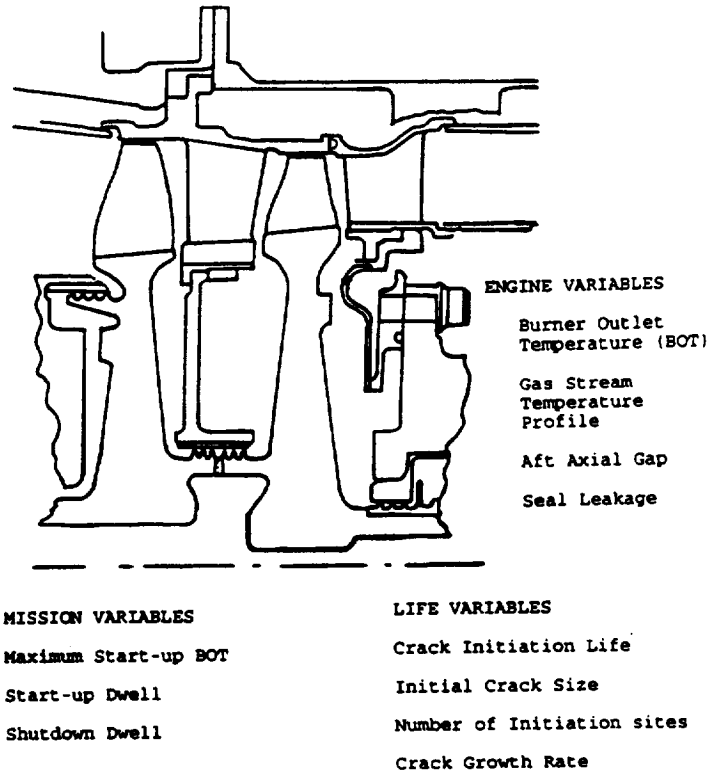

Figure 1: Engine Model Random Variables

stationary parts, and seal leakages. Other variables in the heat transfer model such as idle dwell times are also treated as random variables.

The nominal mission duty cycle was defined after consultation with test pilots. The mission represents starting a cold engine, taking-off, flying to a destination, landing, idling while there, returning, and shutting-down. The heat transfer model is applied at small time increments over the entire mission producing disk temperatures throughout the mission.

The disk stresses and strains throughout the mission are determined using finite element models which incorporate such variables as the disk temperatures, centrifugal forces, and the material properties . The random variables in the structural are the disk temperatures. Figure 2 shows how the mission definition is used to determine the disk stresses.

Both axisymmetric and 3-D finite element models are used in the analysis. The 3-D finite element model is needed to represent the locally complex geometry at the critical location but the 3-D model is too expensive to be used at each instant in time throughout the mission. Therefore, a simplified axisymmetric finite element model is applied at all instances throughout the mission. A rainflow type analysis is used to determine the mission times which define the major and minor stress cycles at the critical location [2]. The 3-D finite element model is used to determine the locally-accurate stresses and strains at the critical mission times.

The crack propagation life is determined using a linear elastic fracture mechanics (LEFM) model based on the crack tip stress intensity factor K. The factor ΔK is determined using the stress cycle and crack

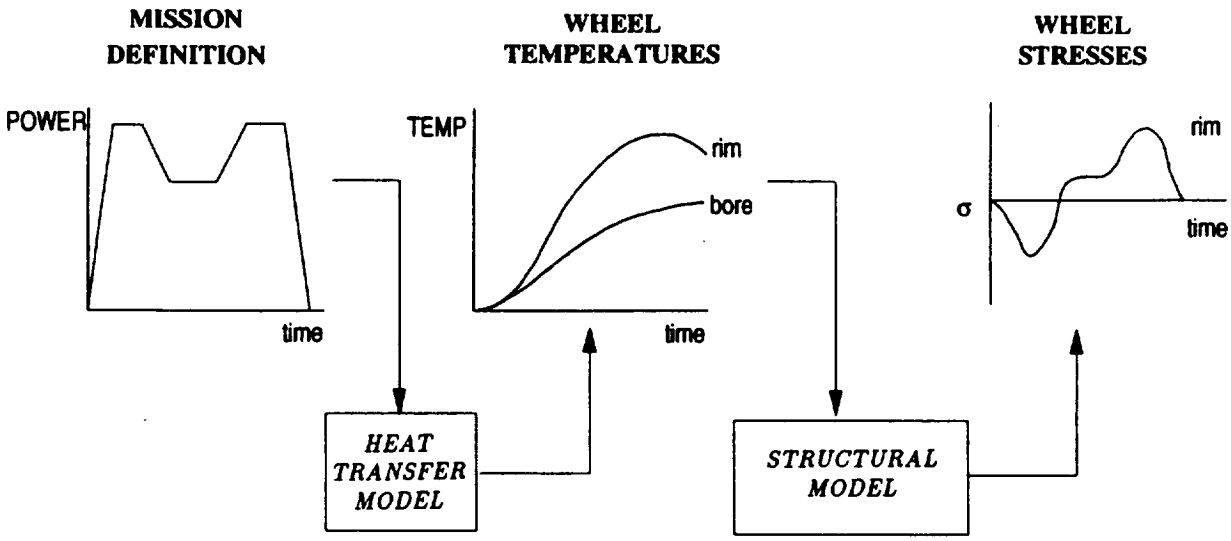

Figure 2: Models Used at All Mission Points

geometry. The model considers disk geometry, initial crack size, and material data. Failure occurs when K exceeds K_{IC}. The Paris law

$$\frac{da}{dN} = C(\Delta K)^n \tag{2}$$

is used to define the crack propagation at a given R and temperature, where $\frac{da}{dN}$ is the crack growth rate, ΔK is the stress intensity factor, and C,n are material constants. The maxima and minima of the stress cycles computed from the mission analysis, the material constants, and the initial crack size are considered random variables.

1.3 Perturbation Analysis

The relationship between the potentially significant random variables and the fatigue life is determined using finite difference perturbation analysis. An analysis is performed using the nominal values of the all random variables to produce the fatigue life for the nominal mission. The analysis is then repeated using the perturbed value of each random variable and the mean value of all the other random variables producing results for a perturbed mission.

Perturbation of the random variables in the heat transfer model showed three random variables to have a significant affect on the disk temperatures: burner outlet temperature (BOT) during start, dwell time at idle during start, and dwell time at idle before shutdown. The stress and subsequent rainflow analysis showed that dwell time at idle during start did not affect the major or minor stress cycles. The fatigue crack propagation analysis showed the crack growth rate material property and the initial crack size to be

NOMINAL MISSION PARAMETERS	
Initial Surface Width	0.03 in.
Initial Crack Depth	0.015 in.
Start BOT	1800 F
C	10.766×10^{-10}
Dwell	120 sec.

	Life (missions)
Nominal Mission	6574
Change BOT	
1900	5487
2000	4227
2100	3077
2200	2478
2300	1971
Change Dwell	
60	6227
180	6723

	Life (missions)
Change C	
$2.2(\times 10^{-9})$	3216
1.8	3931
1.4	5055
0.6	11797
0.24	32083
Change a_i	
0.01	8183
0.02	5641
0.025	5040
0.03	4647

Table 1: Perturbation Analysis Example

significant random variables. Table 1 shows example results for the perturbation analysis.

The rainflow analysis may indicate that some mission points are not important in determining the stress cycles for a particular mission. Care must be used in eliminating these mission points from the analysis because they may be significant for a differently perturbed mission.

1.4 Significant Random Variables

The perturbation analysis showed that six of the eleven potentially significant random variables could be considered deterministic which leaves five significant random variables.

1.4.1 Number of Accumulated Missions

The number of missions accumulated by each disk is a random variable because the engine has both a cyclic and hourly life limit. The cyclic life limit is 3000 missions. The hourly life limit is 1500 hours. The distribution of accumulated cycles at disk retirement and the number of missions on each of the in-service

disks is determined from field service records. The histogram of the number of cycles on the retired disks is added to the histogram of the number of cycles on the in-service disks to produce the histogram of total fleet suspensions. The histogram of total fleet suspensions was approximated with a truncated Weibull distribution.

1.4.2 BOT During Start

The BOT is a function of the duration the start switch is depressed by the pilot. The longer the pilot depresses the switch the higher is the BOT. If the ambient temperature is cold, the engine is mistuned, or the battery is low, the pilot may depress the switch for a long time resulting in high BOT. The high BOT causes a thermal gradient across the disk which results in compressive yielding at the rim. The residual effect of the yielding is to increase the R ratio ($\sigma_{min}/\sigma_{max}$) of subsequent cyclic stresses. The high start BOT affect the disk until a higher start BOT is experienced and the R ratio increases. There is little information available concerning the occurrence of high start BOTs because start BOT is not recorded. The range of possible start BOTs was divided into seven discrete temperatures for convenience. The probability of occurrence of the discrete BOT for each start was estimated by interviewing the engine operators.

FORM analysis cannot account for a time dependent random variable such as start BOT. However, some assumptions can be made about the start BOT that will allow the FORM analysis to compute an upper bound on the P_f. The worst case scenario is to determine the highest BOT the disk ever experiences and assume the high BOT occurs on the first start.

Assume that the disk must endure 3000 missions. The probability of a disk experiencing a start BOT of at least t in 3000 missions is

$$P_{t3000} = 1 - (1 - P_{t1})^{3000} \tag{3}$$

where P_{t1} is the probability of experiencing a BOT of at least t for each start.

The BOT distribution must be converted from a discrete distribution to a continuous distribution before it can be used in FORM analysis. A polynomial curve fit is used to approximate the discrete distribution in the standard normal (z,u) space

$$z = \frac{t - \mu_t}{\sigma_t} \tag{4}$$

$$u = \Phi^{-1}(P(t < T)) \tag{5}$$

where z is the standard variable, u is the standard normal variable, t is the the value of the random variable T representing the start BOT, Φ^{-1} is the the inverse of the standard normal transform and μ_t, σ_t are the mean and standard deviation of the start BOT.

The parameters μ_t and σ_t are estimated using the method of moments. The parameters z and u are computed using Equations 4 and 5. By taking a polynomial curve fit of u in terms of z, the start BOT

distribution can be described by a function of the form

$$u = A_0 + \sum_{i=1}^{n} A_i z^i \tag{6}$$

1.4.3 Dwell Time Before Shutdown

Longer idle dwell times affect the thermal loading by allowing the temperatures to stabilize, thus decreasing the thermal gradient between the disk bore and rim during the shutdown. The dwell time distribution is assumed to be lognormal. The distribution parameters were estimated by interviewing the engine operators.

1.4.4 Initial Crack Size

The crack initiation stage can be broken down into two stages: crack nucleation and small crack growth. The stress concentrations of the complex geometry at the disk rim cause crack nucleation. In nickel-base alloys, planar slip also causes crack nucleation even when no geometric stress concentration is present.

The second phase of crack initiation is the small crack growth phase. A small crack can be thought of as a crack which is small compared to the microstructure. The conventionally cast nickel-based superalloy disk has large grains. Therefore a physically large crack may still be considered microstructurally small because the crack can lie in one or two grains. The crack growth rate of a small crack may vary widely, growing very quickly and then retarding for thousands of cycles. Some cracks completely arrest. Grain size and resistance at the grain boundary affect the small crack growth rate and are both random. In the large grain alloys, a significant amount of the fatigue life can be spent in the small crack regime. A better understanding of crack nucleation and the small crack effect is important in assessing disk fatigue life. Current research of the authors investigates the random behavior of crack initiation.

The available crack initiation models are based on smooth round bar (SRB) tests. SRB tests of large grain are such that after a crack nucleates, it progress to specimen failure in very few cycles. Consequently, the SRB-based crack initiation models are not useful for determining crack growth in the small crack regime but can be used to determine the cycles to crack nucleation. Comparison of the analytical strains from the 3-D stress analysis with the SRB test indicate that crack nucleation will occur in very few cycles.

The procedure in this paper is to assume a crack initiation life of zero cycles, and to choose a range of initial equivalent flaw sizes (EIFS) based on the comparison of the analytical crack growth results with crack size data from disks inspected in the field. The crack size does not represent the physically realized crack initiation size, but is a crack in the LEFM regime that represents the culmination of crack nucleation and the small crack effect. In other words, although the disk may not have a crack size of a_i at zero cycles, the crack growth analysis and field experience indicates that the disk "acts" as though it has a crack of size a_i at zero cycles [3]. The initial crack size is found to fit a Weibull distribution.

The crack initiation size is not an independent random variable, but is highly correlated to start BOT because crack initiation size is a function of the stress ratio R which is a function of start BOT. The FORM

Random Variable	Distribution Type	Mean	Std. Dev.
burner outlet temperature (T)	curve fit	2073^0 F	239^0 F
dwell before shutdown (D)	lognormal	120.5 sec	38 sec
initial crack size (a_i)	Weibull	0.017 in	.00324 in
Paris law coefficient (C)	lognormal	1.02×10^{-9}	0.25×10^{-9}
		Parameters	**Truncation**
Accumulated Missions	Trunc. Weibull	$\theta = 2000$ $\beta = 3$	max = 3000

Table 2: Random Variable Statistics

analysis does not consider the correlation between crack initiation size and start BOT. The fleet simulation does include such correlation.

1.4.5 Crack Growth Rate Properties

The linear elastic fracture mechanics (LEFM) crack growth properties of nickel based superalloy were determined using the data from three compact tension tests. The results from the three tests were fitted to the Paris law (Eq. 2). Crack growth rate is commonly considered a lognormal random variable [4]. In the present study, n was assumed to be constant and C lognormally distributed [5]. Table 2 shows the statistics of the random variables to be used in this paper.

1.5 Regression Analysis

For most realistic structures, the performance function $g(\mathbf{X})$ is generally not available as an explicit, closed-form function of the input variables. The performance function has to be computed through regression analysis of the results of the perturbation analysis. In the present study, the performance function defines fatigue life as a function of the random variables.

$$g(\boldsymbol{X}) = M = f(T, D, a_i, C) \tag{7}$$

where M is the number of missions until failure, T is the start BOT, D is the dwell time before shutdown, a_i is the initial crack size, and C is the crack growth rate for Paris law (Eq. 2). The current analysis uses the response surface approach to construct a polynomial approximation for $g(\mathbf{X})$.

First order reliability analysis assumes a linear approximation of the performance function in standard normal space. If the performance function is highly nonlinear in real space, it is likely to be highly nonlinear in standard normal space and the first order analysis may have convergence problems. Therefore, it is desirable to develop a simple performance function that can be transformed into a linear performance function.

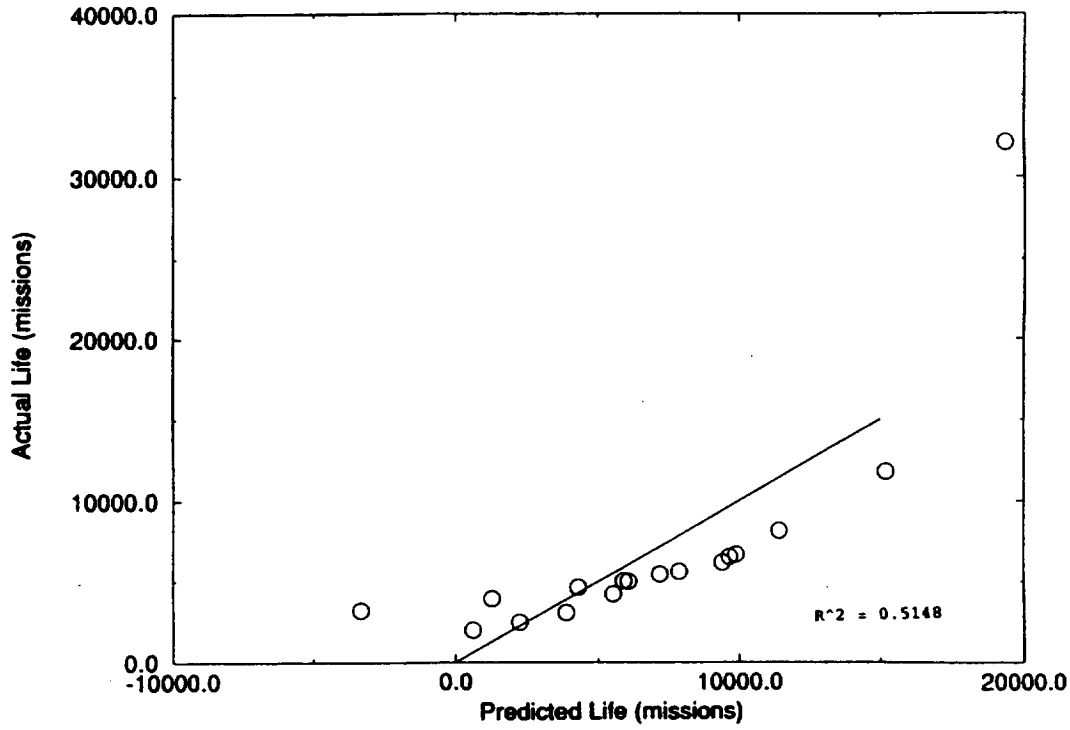

Figure 3: Linear Performance Function Goodness of Fit

1.5.1 Simple Linear Performance Function

Assume the performance function is the simple function

$$M = A_0 + A_1 \cdot (T) + A_2 \cdot (D) + A_3 \cdot (a_i) + A_4 \cdot (C) \tag{8}$$

where the coefficients A_i are determined by performing a least squares fit on the fatigue life perturbation results. Figure 3 shows that simple linear performance function of Equation 8 gives a fairly poor fit ($R^2 = 0.5148$) and a "better" performance function is desired.

1.5.2 Logarithmic Performance Function

Consider the Paris law representation of an edge crack in an infinite plate subjected to a constant stress cycle.

$$\frac{da}{dN} = C\Delta K^n \tag{9}$$

$$\Delta K = \beta\Delta\sigma\sqrt{a} \tag{10}$$

where, a is the crack length, N is the number of cycles, ΔK is the stress intensity factor, $\Delta\sigma$ is the stress range, β is the geometry constant ($1.12\sqrt{\pi}$), and C,n are the material properties. Expanding ΔK and integrating both sides

$$C(\beta\Delta\sigma)^n \int_0^M dN = \int_{a_i}^{a_f} a^{-\frac{n}{2}} da \tag{11}$$

$$M = \frac{a_i^{1-\frac{n}{2}} - a_f^{1-\frac{n}{2}}}{C(\beta\Delta\sigma)^n(\frac{n}{2}-1)}, n \neq 2 \tag{12}$$

where M is the number of mission to failure, a_i is the initial crack size, and a_f is the failure crack size. If $n < 2$ and $a_i \ll a_f$, then $a_i^{1-\frac{n}{2}} \gg a_f^{1-\frac{n}{2}}$ and Equation 12 can be written as

$$M = \frac{a_i^{1-\frac{n}{2}}}{C\Delta\sigma^n(\beta^n(\frac{n}{2}-1))} \tag{13}$$

Taking the log of both sides

$$\log M = -\log(\beta^n(\frac{n}{2}-1)) - \log C - n\log\Delta\sigma + (1-\frac{n}{2})\log a_i \tag{14}$$

Equation 14 is a linear equation of M in log space and can be written as

$$\log M = A_0 + A_1\log C + A_2\log\Delta\sigma + A_3\log a_i \tag{15}$$

Equation 15 suggests that the linear equation in log space

$$\log M = A_0 + A_1\log(T) + A_2\log(D) + A_3\log(a_i) + A_4\log(C) \tag{16}$$

may provide a performance function that more closely fits the results of the fatigue life perturbation analysis. The coefficients A_i are determined by performing a least squares fit on the fatigue life perturbation analysis.

Equation 16 was suggested from the Paris law representation of an edge crack in an infinite plate subjected to a constant stress cycle. Figure 4 shows that a very good fit ($R^2 = 0.9885$) was obtained over a wide range of the random variables even though the crack transitioned from a surface crack to a corner crack to a through crack and was subjected to a complex stress cycle.

2 First Order Reliability Method

The probability of structural failure is estimated through the definition of a limit state corresponding to a failure mode, and by integrating the joint probability density function (*pdf*) of all the random variables over the region where the limit state is violated, as

$$P_f = \int_{g(X)\leq 0} f_X(x)dx \tag{17}$$

where $g(\mathbf{X}) = 0$ represents the limit state, $f_X(x)$ is the joint *pdf* of the random variables $\mathbf{X}$. The difficulty in evaluating the above multi-dimensional integral has led to the development of approximate analytical methods such as first-order reliability methods (FORM).

A first-order approximation to the limit state is shown in Figure 5. The original variables ($\mathbf{X}$) are all transformed to equivalent uncorrelated standard normal variables ($\mathbf{U}$), and the closest point to the origin on the limit state is found. This minimum distance point is in fact the most probable point (MPP) of this limit state. A first-order estimate of the failure probability is obtained as [6]

$$P_f = \Phi(-\beta) \tag{18}$$

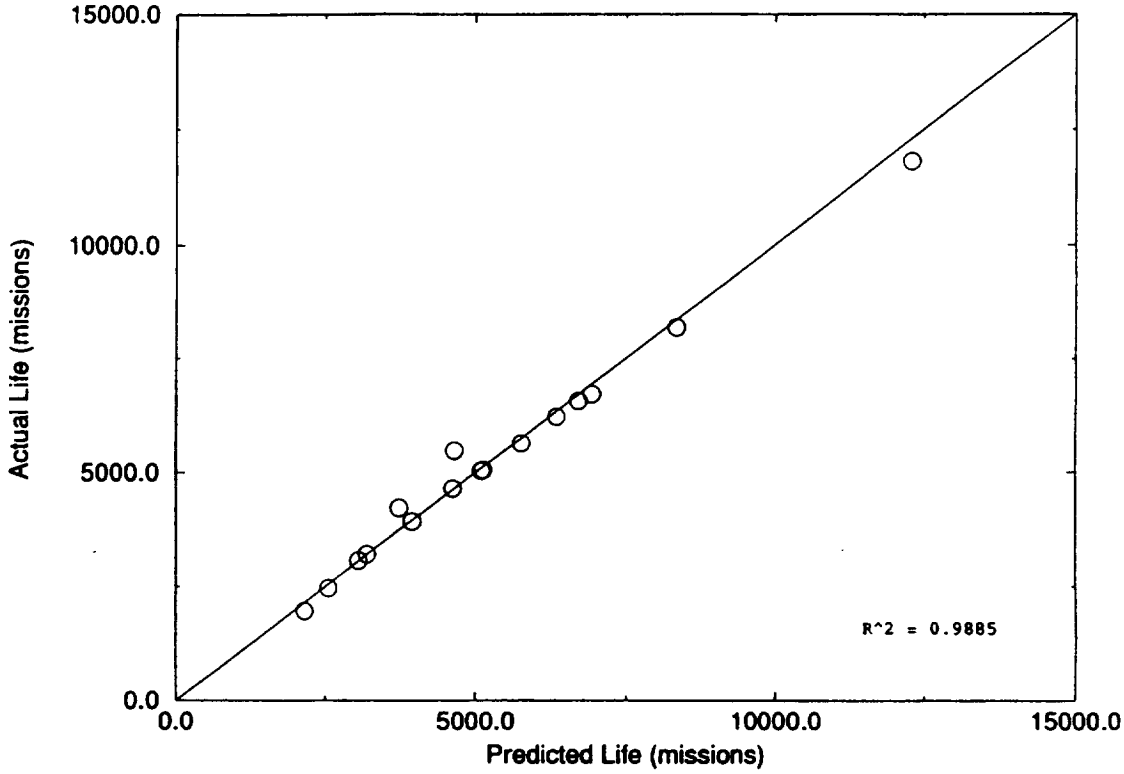

Figure 4: Logarithmic Performance Function Goodness of Fit

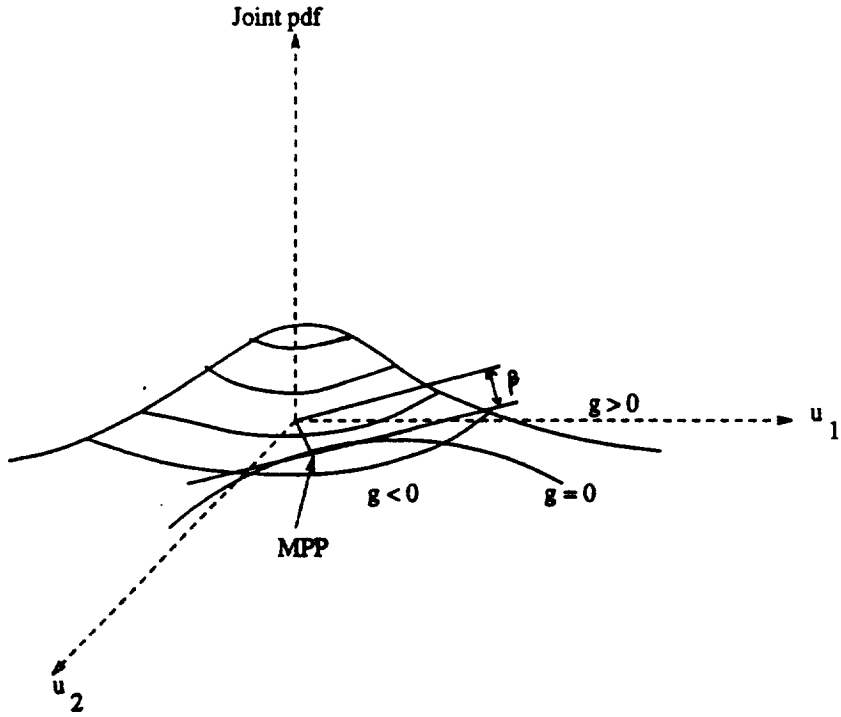

Figure 5: Failure Probability Estimation

where β is the distance from the origin to MPP (referred to as the reliability index), and Φ is the cumulative distribution function of a standard normal variable. Thus the problem of multi-dimensional integration of the joint *pdf* in Equation 17 is transformed to an optimization problem followed by a single dimensional integration of a normal *pdf* due to the linearization of the limit state surface at the MPP. Integration of the normal *pdf* is readily available.

Practical application of the above technique has to include random variables that may be correlated and non-normal. The correlated variables may be transformed to a set of uncorrelated variables through orthogonalization of their covariance matrix [7]. In the case of non-normal variables, it is advantageous to find equivalent normal variables, so that once again the MPP of the limit state can be found in the reduced normal space and Equation 18 can be used. Such a transformation should result in a close approximation to the actual probability content in the failure domain. Equivalent normals can be found with different number of conditions, depending on the accuracy desired.

Rackwitz and Fiessler [8] suggested that at each iteration of the search for the minimum distance point, the cumulative distribution function (*cdf*) and *pdf* of the non-normal variable be equated to the *cdf* and *pdf* of a normal variable, resulting in the computation of mean and variance of the equivalent normal variable. Thus this was a two-parameter approximation. Chen and Lind [9] proposed a three-parameter approximation, by requiring that the slopes of the two *pdf*s should also be equated; the third parameter in this case is a scale factor. Wu and Wirsching [10] refined the three-parameter approximation by minimizing the error sum of squares between the original distribution and the equivalent normal distribution. The motivation for these higher and higher levels of refinement is to find an equivalent normal distribution that very closely matches the original distribution over a wide range of values. Since most of the probability content can be expected to be concentrated in the neighborhood of the MPP, finding a good equivalent normal over a wide range around the MPP may result in a very close approximation to the actual probability content with the use of Equation 18.

The NESSUS/FPI (Nonlinear Evaluation of Stochastic Structures Under Stress/Fast Probability Intergrator) computer code developed at Southwest Research Institute under the leadership of NASA Lewis Research Center [11] is used in the current analysis. NESSUS/FPI uses the refined three-parameter equivalent normal transformation scheme of Wu and Wirsching [10]. However, instead of performing many iterations to search for the exact minimum distance point, NESSUS employs an Advanced Mean Value (AMV) procedure [12] to obtain sufficient accuracy in the second iteration. The ability to make substantial corrections to the reliability estimate in the second iteration derives from the use of information from the previous step. The search begins by computing the sensitivities of the performance function at the mean values of the random variables, and using these sensitivities to obtain a mean value first order (MVFO) estimate of the MPP and failure probability. Reanalysis at this point provides the correct value of the performance function at this point. This information, combined with that from the MVFO analysis, is seen to provide an accurate Advanced Mean Value (AMV) estimate of the failure probability. Further refinements are also possible, if

necessary. The AMV analysis has been verified for numerous problems using Monte Carlo simulation and has been found to provide accurate and fast estimates of failure probability for practical space shuttle main engine (SSME) hardware [13] [14].

A sensitivity analysis defining the relative importance of the random variables can be performed using concepts of the FORM. The sensitivity α of the reliability index β to the random variables $\mathbf{X}$ is a computed through

$$\alpha_i = \frac{\partial \beta}{\partial X_i} = \sum_{j=1}^{n} \frac{\partial \beta}{\partial U_j} \frac{\partial U_j}{\partial X_i} \tag{19}$$

where U_j's are the uncorrelated standard normal variable, and n is the number of random variables. $\frac{\partial U_j}{\partial X_i}$ is available through the transformation from the $\mathbf{X}$ variable to the $\mathbf{U}$ variable. Equation 19 incorporates both the physical sensitivity and the effect of the uncertainty of the random variables. A sensitivity vector is usually constructed by normalizing the values obtained above.

The sensitivities indicate which engine parameters need to be controlled to increase fatigue life. If the fatigue life is found to be insensitive to the variation of certain random variables, then these random variables can be considered deterministic in further analysis. Parametric studies can be performed to determine whether improving the mean value or decreasing the scatter is most beneficial to the design life.

2.1 FORM Analysis Computation

A FORM analysis was performed to determine the fatigue reliability of the first stage disk rim of the high pressure turbine using a logarithmic performance function in the form of Equation 16 and the random variable statistics of Table 2. The computations were performed using NESSUS/FPI [15] with the log transformation [10]. The results of the FORM analysis are shown in Table 3. The P_f and sensitivities of the random variables for three performance levels are reported. The sensitivity analysis combines the relative influence of the random variable with the variation of the random variable to quantitatively access the "importance" of each random variable. The analysis showed the ranking of importance of the random variables to be the same at each of the response levels. The start BOT is the most important, then the crack growth rate, then the initial crack size, and finally, the dwell time before shutdown. The sensitivity of dwell time before shutdown is small compared to the other random variables. Therefore, dwell time before shutdown will be disregarded as a random variable in subsequent analysis.

3 Hybrid Monte Carlo Simulation

Monte Carlo is the process of replicating the response of a system based on a set of assumptions about the random variables and the conceived models of the system. The Monte Carlo simulation relies on random generation of parameter values for each deterministic analysis and estimation of response distribution statistics or reliability based on numerous repetitions. The hybrid Monte Carlo method does not use the

Performance Level (missions)	2000	4250	10000
Probability of Failure	0.079	0.52	0.92
Random Variable	α	α	α
burner outlet temperature (T)	0.802	-0.912	-0.972
dwell before shutdown (D)	-0.0597	0.0389	0.0227
initial crack size (a_i)	0.213	-0.161	-0.100
Paris law constant (C)	0.561	-0.374	-0.213

Table 3: FORM Analysis Results

computationally extensive system, structural, and fatigue models for each simulation. A computationally efficient scheme is developed using a series of fatigue crack growth functions derived from the results of the perturbation analysis.

A fleet simulation is performed to predict P_f and the number of mission on the failed wheels using the hybrid Monte Carlo method. The fleet simulation allows for variations in the initial crack size, the crack growth rate and the number of accumulated missions. The discrete time dependence of the start BOT is incorporated without worst case assumptions used in the FORM analysis.

A flow diagram for the fleet simulation is shown in Figure 6. The overall flow of the simulation will be discussed first. Discussion of the details of the steps will follow.

The input to the simulation consists of

1. Initial crack size (a_i) distribution
2. High start BOT initial crack size scale factor (CIF)
3. Crack growth function (f)
4. Crack growth rate (CGR) distribution
5. Failure crack size (a_f)
6. Missions before retirement (M_r) distribution
7. Mission step size (dM)
8. Number of disks to be simulated (NSIM)

The simulation chooses a random disk by generating the values for a_i, cgr and M_r, and also generates a start BOT value. The crack growth function is used to determine the crack size a and the total number of missions M after dM cycles. The simulation compares a to a_f and M to M_r. If $a > a_f$, the disk fails,

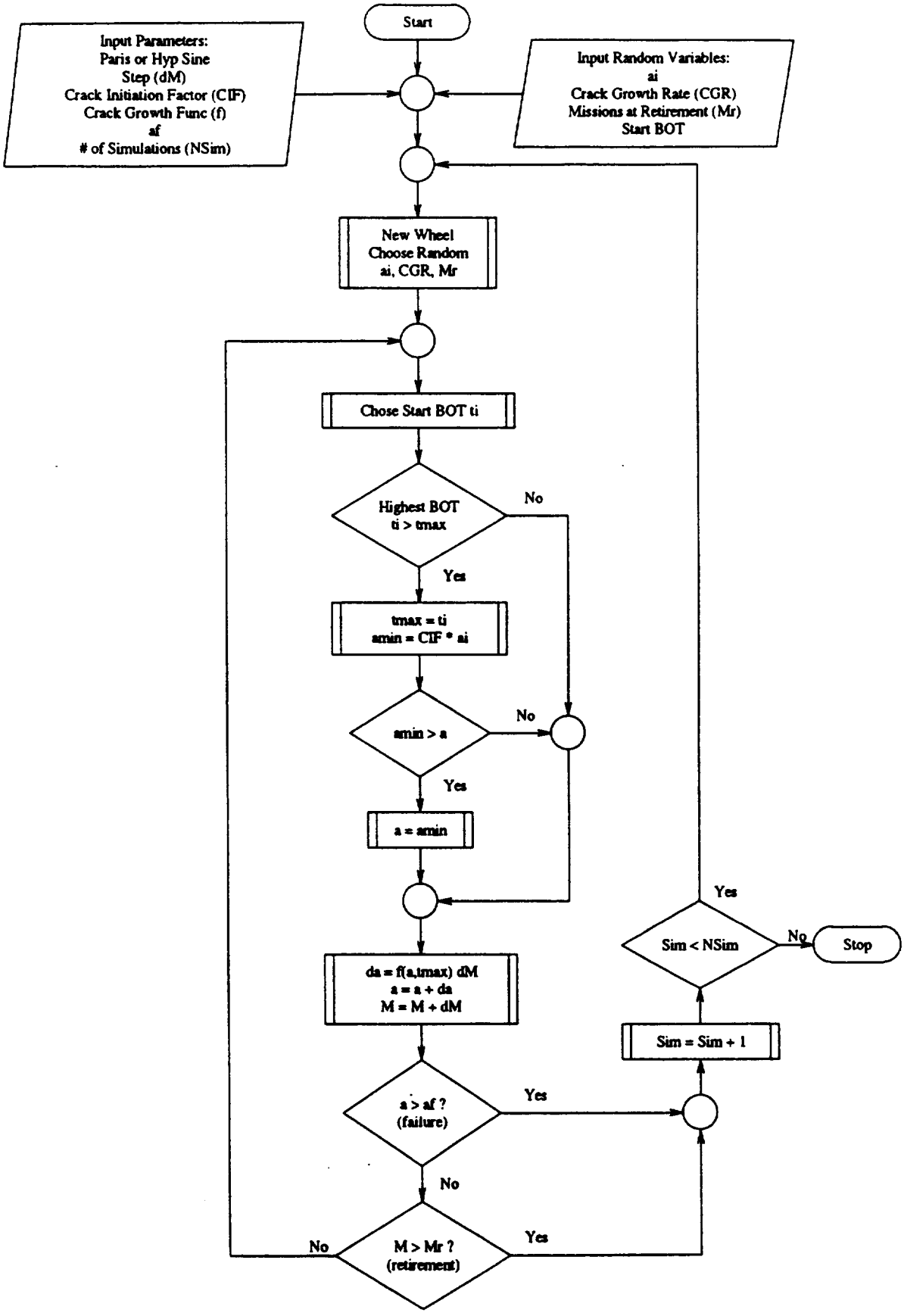

Figure 6: Fleet Simulation Flow Chart

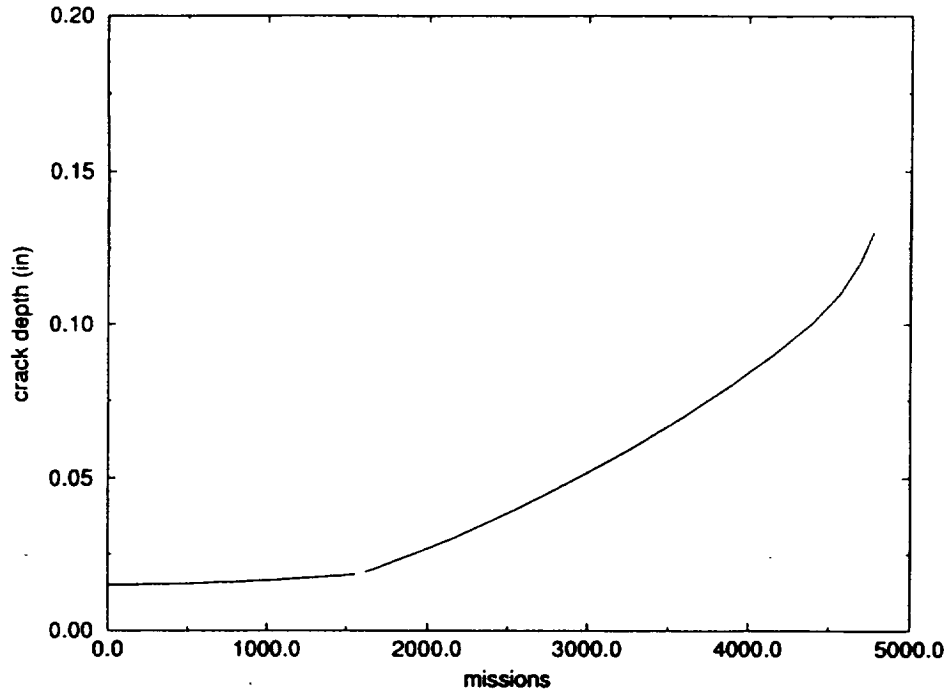

Figure 7: Crack Growth using Engine Models

the failure is counted, the missions to failure is stored and a new disk is chosen. If $M > M_r$, the disk is retired and a new disk is chosen. If $a < a_f$ and $M < M_r$, a new start BOT t_i is chosen. If t_i is higher than any previous start BOT, then $t_{max} = t_i$, and a_{min} is calculated and compared with a. If $a_{min} > a$, then $a = a_{min}$. The crack growth function uses the new a and t_{max} to determines the crack size and number of accumulated mission. The disk is again checked for failure or retirement or the disk continues. The simulation is repeated for many disks. A computer program FLEETSIM was developed to perform the fleet simulation.

3.1 Simulating the Crack Growth

Use of a computationally extensive engine models to determine the crack growth for each simulation would be prohibitively expensive. Therefore a series of closed-form equations of crack growth rate as a function of crack size and start BOT were developed. The equations were derived by fitting a polynomial equation to the results from the perturbation analysis for each start BOT.

For example, in the perturbation analysis of start BOT, the engine models were used to calculate the crack size versus missions for the nominal start BOT using the mean initial crack size and mean crack growth rate. The data is plotted in Figure 7. The crack growth rate at any mission M_i can be approximated by

$$\frac{da}{dM} = \frac{a_{i+1} - a_i}{M_{i+1} - M_i} \tag{20}$$

The crack growth rate is calculated over a range of missions and plotted in log space as shown in Figure 8 which shows two disjointed regions. The points in the first region represent the crack growth rate while

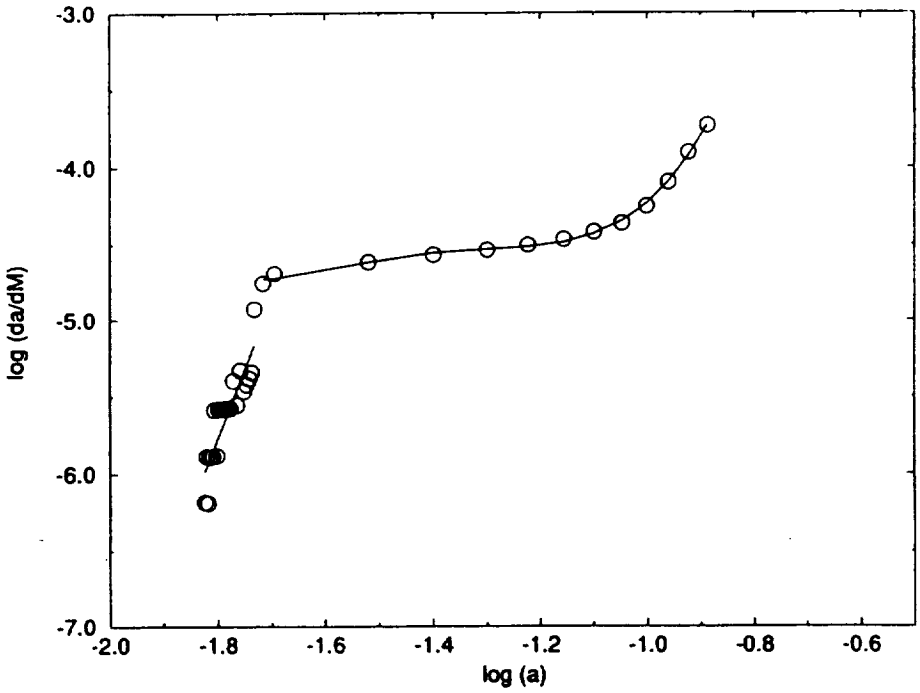

Figure 8: Crack Growth Rate Derived from Engine Models

the crack is a surface crack and points in the second region represent the crack growth rate for the crack after it has transitioned to a corner crack. The closed-form equation for crack growth rate is approximated by fitting a polynomial equation to the points.

$$\log \frac{da}{dM} = \sum_{i=0}^{n} A_i (\log a)^i \tag{21}$$

Two equations are needed, one valid for the first range and the other valid for the second range. The polynomial fits are shown in Figure 8. A different set of equations is determined from the perturbation analysis for each start BOT.

The crack growth for any crack size and any start BOT can be determined by

$$da = f(a, t_{max}) dM \tag{22}$$

$$f(a, t_{max}) = \log^{-1}(\sum_{i=0}^{n} A_i(a, t_{max})(\log a)^i) \tag{23}$$

where da is the crack growth in dM missions, a is the previous crack size, t_{max} is the maximum start BOT experienced, dM is the mission step size, and $A_i(a, t_{max})$ is the crack growth function coefficients. Knowing the initial crack size, the crack size a at missions M can be approximated by

$$da = f(a, t_{max}) dM \tag{24}$$

$$a = a + da \tag{25}$$

$$M = M + dM \tag{26}$$

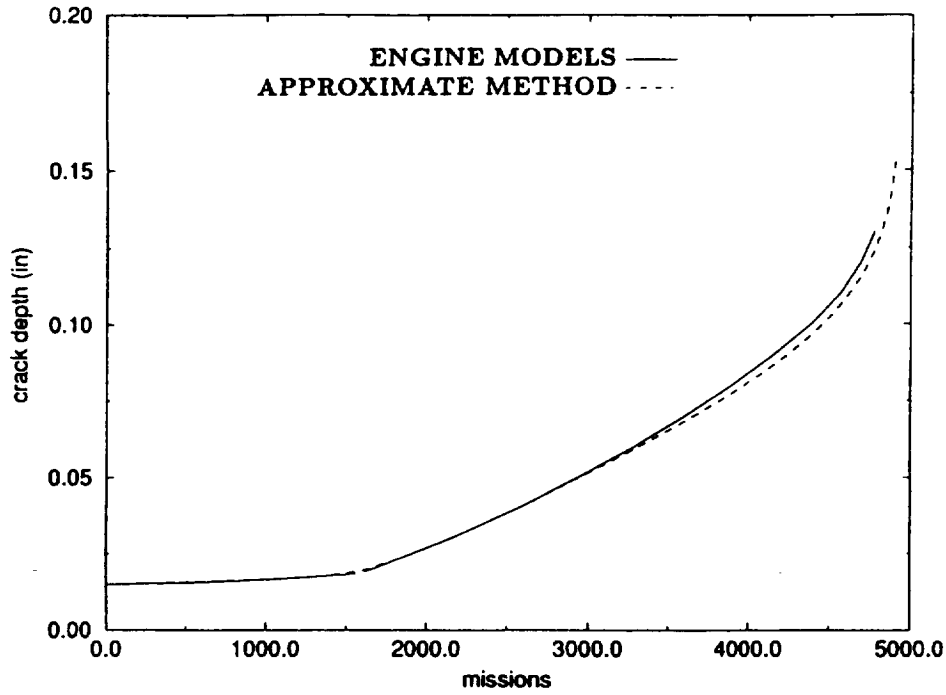

Figure 9: Crack Growth: Engine Model vs. Approximate Method

The function $f(a, t_{max})$ allows the start BOT to increase at any mission. The accuracy of the above approximation can be verified by comparing the results of the approximation with the engine model results for the same initial crack size and start BOT as shown in Figure 9.

3.1.1 Step Size

A mission step size parameter dM has been introduced to make the simulation computationally more efficient. Using the mission step size enables one computation to determine the crack growth for a group of missions instead of a crack growth computation for each mission.

The *cdf* of start BOT for each start must be converted to the *cdf* of start BOT for dM missions. The probability of a disk experiencing a BOT of at least t_i in dM starts is

$$\Psi_{tdM} = 1 - (1 - \Psi_{t1})^{dM} \tag{27}$$

where Ψ_{tdM} is the probability of experiencing a BOT of at least t in dM starts, and Ψ_{t1} is the probability of experiencing a BOT of at least t_i for each start. Figure 10 shows the results of the approximate method as dM is increased. The results are acceptable even when dM is greater than 1% of total life.

3.1.2 High BOT Initial Crack Size Factor

As discussed earlier, to correlate the crack growth analysis with the early field failures, a large initial crack size must be correlated with high start BOT occurring early in life. The initial crack size is the effective

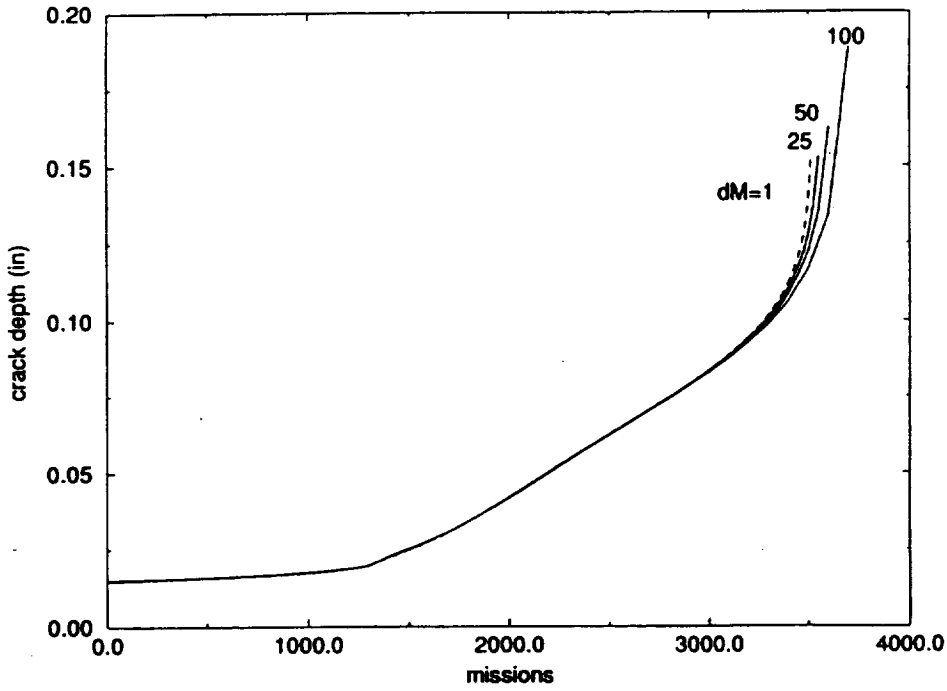

Figure 10: Approximate Method Step Size Study

crack size after the crack initiation phase. The initial crack size is not a manufacturing defect before the disk enters service. The large initial crack size to high start BOT correlation is incorporated by scaling the initial crack size by a crack initiation factor.

$$a_{min} = CIF_{tmax} a_i \tag{28}$$

where a_{min} is the minimum crack size after a start BOT of t_{max}, CIF_{tmax} is the scaling factor for a start BOT of t_{max}, and a_i is the initial crack size. When the disk experiences a new maximum start BOT, a_{min} is calculated and compared to the current crack size a. If a_{min} is greater than a, then the current crack size is set equal to a_{min}.

3.1.3 Random Crack Growth Rate

The crack growth rate will change for each simulated disk. However, the crack growth function, $f(a, t_{max})$, defined by the coefficients A_i in Figure 8 was derived from mean crack growth rate analyses. The crack growth function must be adjusted for different crack growth rates.

A different crack growth rate $CGR1$ is incorporated by adjusting the crack growth function.

$$f(a, t_{max})_{cgr1} = \frac{C_{cgr1}}{C_{mean}} (f(a, t_{max})_{mean}) \tag{29}$$

where $f(a, t_{max})_{cgr1}$ is the crack growth function for a crack growth rate of $cgr1$, $f(a, t_{max})_{mean}$ is the crack growth function for the mean crack growth rate, C_{cgr1} is the Paris Law coefficient for a crack growth rate of $cgr1$, and C_{mean} is the Paris Law coefficient for the mean crack growth rate.

# of failures out of 100,000 disks	650
# of failed disks	# of missions
13	0 - 499
111	500 - 999
149	1000 - 1499
129	1500 -1999
144	2000 - 2499
104	2500 - 3000

Table 4: Fleet Simulation Results

3.2 Necessary Number of Simulations

The number of necessary simulations can be determined by [16]

$$\% \text{ error} < 200\sqrt{\frac{1-P_f}{NSIM \cdot P_f}} \tag{30}$$

where % error is the percent error in P_f (with 95% confidence), and $NSIM$ is the number of simulations.

3.3 Fleet Simulation Results

Simulation of 100,000 disks was performed using the above method and the random variable statistics discussed earlier. The fleet simulation determined the P_f and the number of missions on the failed disks as shown in Table 4. A Weibull analysis [17] where the Weibull distribution is defined as

$$P_f = 1 - exp\left(\frac{M}{\eta}\right)^{\zeta} \tag{31}$$

was performed on the results in Table 4. The simulated fleet has a Weibull characteristic life η of 19300 missions and a Weibull slope ζ of 2.14.

The Weibull analysis shows a median disk life of about 15000 missions for the fleet simulation while the FORM analysis showed a median disk life of about 4200 missions. The fleet simulation included the correlation of large crack initiation size with early high start BOT which would tend to reduce the fatigue life. However, the fleet simulation did not assume that the highest start BOT experienced by the disk occurred during the first mission as was done in the FORM analysis. This would tend to increase fatigue reliability. The random variable sensitivities shown in Table 3 indicate that fatigue life is much more sensitive to start BOT than initial crack size, therefore it would be expected that the fleet simulation would show higher disk reliability than the FORM results.

4 System Failure

System failure may occur due to a combination of any of the individual component failure modes. In the simplest case, system failure is simply a series combination of individual failure modes, i.e., violation of any one to the design limit states causes system failure. The reliability of each of the individual failure modes can be determined using the FORM analysis described earlier. Once the failure probabilities for the individual failure modes are computed, the determination of the probability of the union of all the failure modes is a difficult problem. Consider the probability of union of three failure events A, B, and C, defined as

$$\begin{aligned} P(A \cup B \cup C) &= P(A) + P(B) + P(C) - \\ & \quad P(AB) - P(BC) - P(AC) + P(ABC) \end{aligned} \tag{32}$$

where $P(AB)$ refers to the joint probability of A and B. Other joint probability terms are similarly obvious from the equation. Since it is difficult to determine the joint probabilities of more than two failures, several approximate bounds have been proposed for the system failure probability. The simplest among these are Cornell's first-order bounds [18]:

$$\max_{1 \le i \le n} P(E_i) \le P(\cup_{i=1}^{n} E_i) \le \sum_{i=1}^{n} P(E_i) \tag{33}$$

where $P(E_i)$ is the probability of failure of the ith component. The above first-order bounds could be quite large; for accurate estimation, second-order bounds are used. These include the second-order terms in Equation 32, i.e., the joint probabilities of two events. Various second-order bounds are available in literature [19], and their accuracy depends on the ranking of failure modes in the order of decreasing probability. Cruse et al [20] derived second-order bounds which are independent of such ranking. The upper bound is

$$P_S = P(\cup_{i=1}^{n} E_i) \le \left\{ \sum_{i=1}^{n} P(E_i) - \max \left[\sum_{i=2}^{n} \max_{j<i} P(E_i E_j), \max_{1 \le i \le n} \sum_{j=1, j \ne i}^{n} P(E_i E_j) \right] \right\} \tag{34}$$

where P_S is system failure probability. The lower bound is

$$P_S = P(\cup_{i=1}^{n} E_i) \ge \max_{1 \le j \le n} \left\{ P(E_j) + \sum_{i=1, i \ne j}^{n} \max \left[(P(E_i) - \sum_{k=1, k \ne i}^{\max(i,j)} P(E_i E_k)); 0 \right] \right\} \tag{35}$$

In order to use the above second-order bounds, the joint probability of two events $P(E_i E_j)$ needs to be estimated. A first-order approximation to the joint probability was constructed by Ditlevsen [19]; this method is illustrated geometrically in Fig. 11 for two linear limit states. The individual failure mode probabilities in the first-order analysis are determined as

$$P_i = \Phi(-\beta_i) \tag{36}$$

Let each limit state be represented as

$$M_i = \beta_i + \sum_{r=1}^{m} \alpha_r u_r \tag{37}$$

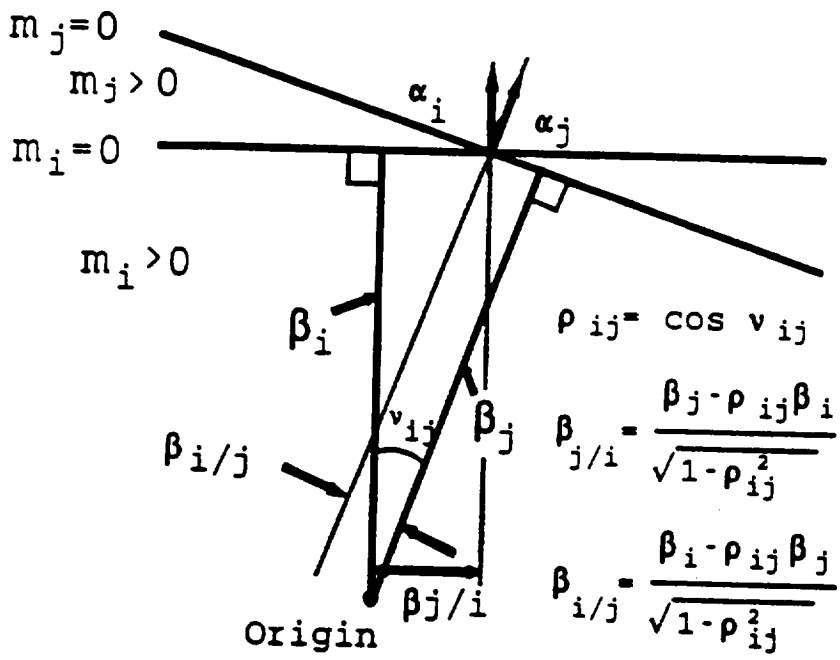

Figure 11: Joint Probability of Two Failure Modes

where m is the number of random variables. The angle between the two limit states provides information about the correlation between the two failure modes. Thus, the correlation coefficient is obtained as

$$\rho_{ij} = \sum_{r=1}^{m} \alpha_{ir}\alpha_{jr} = \cos\nu_{ij} \tag{38}$$

Once β_i, β_j, and ρ_{ij} are known, the joint P_f can be accurately calculated using the integration method developed by Cruse et al [20]. Then the second-order bounds in Equations 34 and 35 can be used to compute the second-order bounds for system failure probability.

4.1 Probabilistic System Sensitivity Factors

As discussed earlier,the influence of various uncertainties on the individual failure modes is a by-product of MPP estimation. The components of the unit gradient vector (i.e., direction cosines) of the limit state at the MPP provide the sensitivity factors for individual failure modes. The sensitivity factors combine the information on both the physical influence and the randomness of the uncertain parameters.

The vector to the individual event (denoted by i) most probable points $(MPP)_i$ is defined with magnitude β_i and direction cosines which are the probabilistic sensitivity factors α_{ij}. The sensitivity factors combine the local physical sensitivities $\partial g/\partial x_j$, as well as the variances, σ_j for each independent random variable.

A first-order approximation to the system sensitivity factors is computed by applying the chain rule of differentiation to the first-order upper bound of system failure probability. This is expressed as

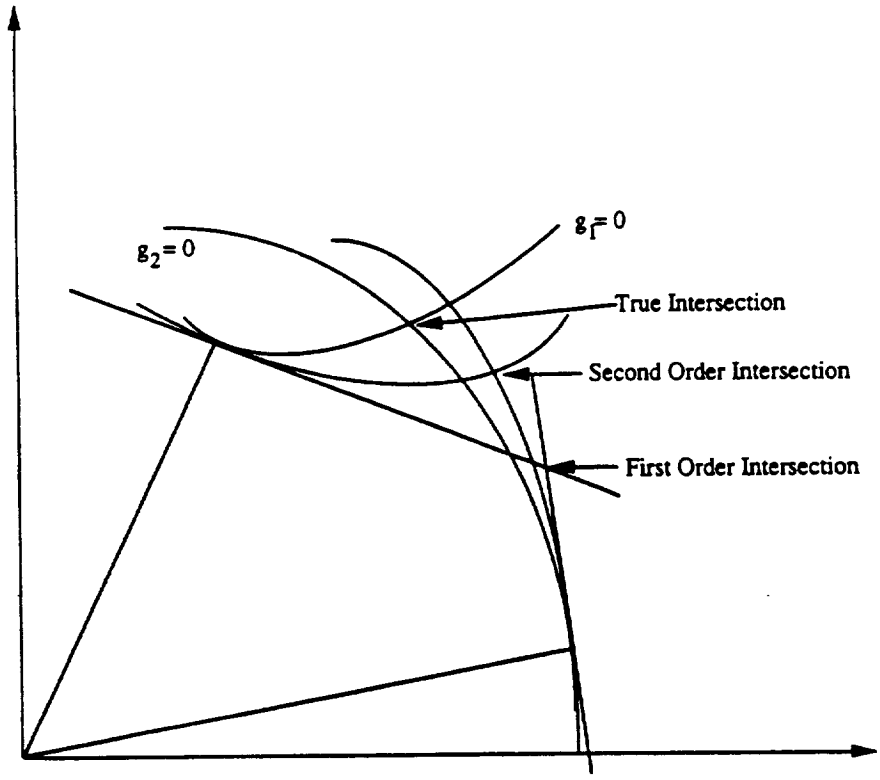

Figure 12: Two Nonlinear Limit States

$$\alpha_j^s = \sum_{i=1}^{n} \alpha_{ij} \phi(\beta_i) \tag{39}$$

where n is the number of component limit states, and j is the random variable number. The α_j^s are normalized with respect to the square root of the sum of the squares of their values, to give a unit system sensitivity vector.

4.2 Nonlinear Limit States

The method described above provides accurate results for linear limit states. However, if the limit states are nonlinear, the joint probability region is different, as illustrated by Fig. 12. In such cases, one needs to find the exact intersection between the two limit states and then estimate the joint probability by constructing linear approximations to the limit states at this intersection, which may be referred to as a joint MPP. The problem of finding the intersection is one of constrained minimization. A simple extension of the well-known Rackwitz-Fiessler algorithm [8] to determine the joint MPP of two nonlinear limit states is outlined in [21].

4.3 System Reliability Example

Consider the two stage high pressure turbine in Figure 1 with fatigue failure modes at four locations: the rim of first stage disk, the bore of first stage disk, the rim of second stage disk, and the bore of the second stage disk. Assume that the crack growth incurred at any location does not effect the damage at the other locations. Also assume that a failure at any location will cause system failure.

Random Variable	Distribution Type	Mean	Std. Dev.
burner outlet temperature (T)	curve fit	2073^0 F	239^0 F
dwell before shutdown (D)	lognormal	120.5 sec	38 sec
1^{st} stage rim initial crack size (a_{1i})	Weibull	0.017 in	.00324 in
1^{st} & 2^{nd} stage bore initial crack size (a_{2i})	Weibull	0.01 in	0.003 in
2^{nd} stage rim initial crack size (a_{3i})	Weibull	0.011 in	0.00283 in
1^{st} stage rim Paris coefficient (C_1)	lognormal	1.02×10^{-9}	0.25×10^{-9}
1^{st} stage bore Paris coefficient (C_2)	lognormal	0.443×10^{-9}	0.25×10^{-9}
2^{nd} stage rim Paris coefficient (C_3)	lognormal	1.05×10^{-9}	0.25×10^{-9}
2^{nd} stage bore Paris coefficient (C_4)	lognormal	0.448×10^{-9}	0.25×10^{-9}
upstream seal clearence (δ)	normal	0.1 in	0.03 in

Table 5: Random Variable Statistics for System Analysis

The failure mode of the first stage rim is influenced by four random variables; start BOT (T), idle dwell time before shutdown (D), crack initiation size (a_{1i}), and Paris law material constant (C_1). The first stage bore is influenced by four random variables; T, a_{2i}, C_2, and an upstream seal clearance δ. The second stage rim in influenced by three random variables; T, a_{3i}, and C_3. The second stage bore is influenced by four random variables; T, the same crack initiation size as the first stage bore a_{2i}, C_4, and the same upstream seal clearance δ as the first stage. The random variable statistics are shown in Table 5.

Using the methods described earlier, a performance function in the form of Equation 16 was developed for each of the four locations. At each location, the performance function and the pertinent random variables were used to perform a FORM analysis for each failure mode individually.

The FORM analysis results for all four failure mode are used to produce the second-order bounds on the system failure probability and the system sensitivities. The P_f and the sensitivities to the random variables of the individual failure modes, as well as the P_f and the sensitivities to the random variables of the system failure are summarized in Table 6. System failure with discrete time-dependent random variables is not considered in this paper. However, system failure with discrete time-dependent random variables would be addressed by a simple extension of the hybrid Monte Carlo method presented.

Summary

This paper described a methodology for probabilistic assessment of the fatigue life of a high pressure turbine subjected to a complex load history.

A logarithmic performance function was derived by performing a regression analysis on the results of the

	Rim 1	Bore 1	Rim 2	Bore 2	System
Probability of Failure	0.077	0.155	0.335	0.68×10^{-7}	1^{st} order bounds 0.355 — 0.567 2^{nd} order bounds 0.479 — 0.483
Random Variable	α	α	α	α	α
T	-0.9715	0.3	-0.2122	0.3272	-0.9517
D	0.0227				0.0232
a_{1i}	-0.1000				-0.1026
C_1	-0.2134				-0.2181
a_{2i}		0.8993		0.834	0.1677
C_2		0.2620			0.0489
δ		0.1808		0.1074	0.0337
a_{3i}			-0.9720		-0.0633
C_3			-0.0102		-0.0661
C_4				0.4310	6.3×10^{-7}

Table 6: System Reliability Analysis Results

engine model perturbations. The methodology incorporated the same basic engine models, including heat transfer, structural, and crack growth models, used in a deterministic fatigue life analysis. The performance function yielded a good approximation of fatigue life over a wide range of the random variables.

First order reliability methods (FORM) were used to compute the probability of failure P_f and sensitivity of the fatigue life to the engine parameters for the first stage turbine disk rim for three performance levels. The sensitivity analysis showed the burner outlet temperature (BOT) to be the random variable to which the fatigue life was most sensitive, indicating that concentrating engineering resources on reducing the mean value and/or reducing the scatter of BOT may be the most efficient way to increase fatigue life.

A discrete time-dependent random variable capability was developed using a hybrid Monte Carlo method. The computationally intensive engine models were not used directly in the Monte Carlo simulation. Instead, the Monte Carlo simulation used a computationally efficient, approximate crack growth function derived by performing a regression analysis on the results of the engine model perturbations.

A computational method was to used determine the system P_f of the overall high pressure turbine. The probabilities for four individual failure modes were computed using FORM. System failure was defined as the union of the individual failure modes. The probability of this union was computed though first and second

order bounds. The method also provided sensivity information about the effect of each random variable on the individual failure probabilities as well as the system failure probability. The burner outlet temperature (BOT) was found to be the random variable to which the fatigue life of the overall turbine was most sensitive.

Acknowledgments - This work was partially supported by NASA contract NAS3-24389, Lewis Research Center, Dr. C. C. Chamis, Program Manager; NASA GSRP Project NGT-51053, Lewis Research Center, Dr. C. C. Chamis, Technical Advisor; and Allison Gas Turbine contract H135571, Dr. J. E. Pope, Project Engineer.

References

[1] Cruse, T.A., Mahadevan, S., Tryon, R.G., "Fatigue Reliability of Gas Turbine Engines, Part I - Methodologies Developed", **Engineering Fracture Mechanics**, under review.

[2] Socie, D.F. and Kuranth, P., "Cycle Counting for Variable Amplitude Crack Growth", **Fracture Mechanics: Fourteenth Symposium, Vol 2**, ASTM STP 791, 1983, pp II-19 – II-32.

[3] Asquith G. and Pickard A.C.,"Fatigue Testing of Gas Turbine Components", **High Temperature Technology, Vol 6**, No 3, August 1988, pp 131-143.

[4] Yang, J.N., Salivar, G.C., Annis, C.G., **Statistics of Crack Growth in Engine Materials - Volume 1: Constant Amplitude Fatigue Crack Growth at Elevated Temperatures**, AFWAL-TR-82-4040.

[5] Provan, J.W., **Probabilistic Fracture Mechanics and Reliability**, Martinus Nijhoff, Dordrecht, The Netherlands, 1987.

[6] Hasofer, A.M. and Lind, N.C., "Exact and Invariant Second Moment Code Format", **Journal of the Engineering Mechanics Division, ASCE, Vol 100**, No.EM1, pp. 111-121, 1985

[7] Ang, A. H.-S. and Tang, W.H., **Probability Concepts in Engineering Planning and Design**, Vol 2, John Wiley and Sons, New York, 1975.

[8] Rackwitz, R. and Fiessler, B, "Structural Reliability Under Combined Random Load Sequences", **Computers and Structures. Vol. 9**, No. 5, pp. 484-494, 1978.

[9] Chen, X., and Lind, N.C., "Fast Probability Integration by Three-Parameter Normal Tail Approximation", **Structural Safety, Vol. 1**, pp. 269-276, 1983.

[10] Wu, Y.T., and Wirsching, P.H., "New algorithm for structural reliability estimation", **Journal of Engineering Mechanics, ASCE, Vol. 113**, No. 9, pp. 1319-1336, 1987.

[11] Cruse, T.A., Chamis, C.C., and Millwater, H.R., "An Overview of the NASA(LeRC)-SwRI Probabilistic Structural Analysis (PSAM) Program", **Proceedings, 5th International Conference on Structural Safety and Reliability (ICOSSAR)**, San Francisco, California, pp. 2267-2274, 1989.

[12] Wu, Y.T., Millwater, H.R., and Cruse, T.A., "An Advanced Probabilistic Structural Analysis Method for Implicit Performance Functions", **AIAA Journal, Vol. 28**, No. 9, pp. 1663-1669, 1990.

[13] Cruse, T.A., Burnside, O.H., Wu, Y.-T., Polch, E.Z., and Dias, J.B., "Probabilistic Structural Analysis Methods for Select Space Propulsion System Structural Components (PSAM)", **Computers and Structures, Vol. 29(5)**, pp. 891-901, 1988.

[14] Rajagopal, K.R., Debchaudhury, A., and Newell, J.F., "Verification of NESSUS Code on Space Propulsion Components", **Proceedings, 5th International Conference on Structural Safety and Reliability, ICOSSAR '89**, San Francisco, California, pp. 2299-2306, 1989.

[15] "NESSUS Reference Manual," Version 1.0, July 1991, Southwest Research Institute, TX.

[16] Ang, A. H.-S. and Tang, W.H., **Probability Concepts in Engineering Planning and Design**, Vol 2, John Wiley and Sons, New York, 1975.

[17] Abernethy, R.B., Breneman, J.E., Medlin, C.H., Reinman, G.L., **Weibull Analysis Handbook**, AFWAL-TR-83-2079, November 1983.

[18] Cornell, C.A., "Bounds on the Reliability of Structural Systems", **Journal of the Structural Division, ASCE, Vol. 93**, No. ST1, pp. 171-200, 1967.

[19] Ditlevsen, O., "Narrow Reliability Bounds for Structural Systems", **Journal of Structural Mechanics, Vol. 3**, 453-472, 1979.

[20] Cruse, T.A., Huang, Q., Mehta, S., and Mahadevan, S., "System Reliability and Risk Assessment", **Proceedings of the 33rd AIAA/ASME/ASCE/AHS/ASC Conference on Structures, Structural Dynamics and Materials**, Dallas, Texas, pp.424-431, 1992.

[21] Mahadevan, S., and Cruse, T.A., "An Advanced First-Order Method for System Reliability," **Proceedings of the ASCE Joint Specialty Conference on Probabilistic Mechanics and Structural and Geotechnical Reliability**, Denver, Colorado, pp. 487-490, 1992.

REPORT DOCUMENTATION PAGE

Form Approved
OMB No. 0704-0188

1. AGENCY USE ONLY (*Leave blank*)	2. REPORT DATE	3. REPORT TYPE AND DATES COVERED
	October 1997	Final Contractor Report

4. TITLE AND SUBTITLE

Fatigue Reliability of Gas Turbine Engine Structures

5. FUNDING NUMBERS

WU–523–22–13–00
NGT–51053

6. AUTHOR(S)

Thomas A. Cruse, Sankaran Mahadevan, and Robert G. Tryon

7. PERFORMING ORGANIZATION NAME(S) AND ADDRESS(ES)

Vanderbilt University
Nashville, Tennessee 37240–0001

8. PERFORMING ORGANIZATION REPORT NUMBER

E–10951

9. SPONSORING/MONITORING AGENCY NAME(S) AND ADDRESS(ES)

National Aeronautics and Space Administration
Lewis Research Center
Cleveland, Ohio 44135–3191

10. SPONSORING/MONITORING AGENCY REPORT NUMBER

NASA CR—97-206215

11. SUPPLEMENTARY NOTES

Project Manager, Christos C. Chamis, Research and Technology Directorate, NASA Lewis Research Center, organization code 5000, (216) 433–3252.

12a. DISTRIBUTION/AVAILABILITY STATEMENT

Unclassified - Unlimited
Subject Category: 24 Distribution: Nonstandard

This publication is available from the NASA Center for AeroSpace Information, (301) 621–0390.

12b. DISTRIBUTION CODE

13. ABSTRACT ***(Maximum 200 words)***

The results of an investigation are described for fatigue reliability in engine structures. The description consists of two parts. Part I is for method development. Part II is a specific case study. In Part I, the essential concepts and practical approaches to damage tolerance design in the gas turbine industry are summarized. These have evolved over the years in response to flight safety certification requirements. The effect of non-destructive evaluation (NDE) methods on these methods is also reviewed. Assessment methods based on probabilistic fracture mechanics, with regard to both crack initiation and crack growth, are outlined. Limit state modeling techniques from structural reliability theory are shown to be appropriate for application to this problem, for both individual failure mode and system-level assessment. In Part II, the results of a case study for the high pressure turbine of a turboprop engine are described. The response surface approach is used to construct a fatigue performance function. This performance function is used with the first order reliability method (FORM) to determine the probability of failure and the sensitivity of the fatigue life to the engine parameters for the first stage disk rim of the two stage turbine. A hybrid combination of regression and Monte Carlo simulation is to use incorporate time dependent random variables. System reliability is used to determine the system probability of failure, and the sensitivity of the system fatigue life to the engine parameters of the high pressure turbine. The variation in the primary hot gas and secondary cooling air, the uncertainty of the complex mission loading, and the scatter in the material data are considered.

14. SUBJECT TERMS

Damage tolerance; Fracture mechanics; Crack initiation; Crack growth; Limit state failure modes; Response surface; First-order reliability; Failure sensitivities; Monte Carlo

15. NUMBER OF PAGES

61

16. PRICE CODE

A04

17. SECURITY CLASSIFICATION OF REPORT	18. SECURITY CLASSIFICATION OF THIS PAGE	19. SECURITY CLASSIFICATION OF ABSTRACT	20. LIMITATION OF ABSTRACT
Unclassified	Unclassified	Unclassified	